



Article

# Design, Synthesis and Evaluation of Novel Molecular Hybrids between Antiglaucoma Drugs and H<sub>2</sub>S Donors

Rosa Sparaco <sup>1</sup>, Valentina Citi <sup>2</sup>, Elisa Magli <sup>3</sup>, Alma Martelli <sup>2</sup> , Eugenia Piragine <sup>2</sup> , Vincenzo Calderone <sup>2</sup>,  
Giorgia Andreozzi <sup>1</sup>, Elisa Perissutti <sup>1</sup> , Francesco Frecentese <sup>1</sup> , Vincenzo Santagada <sup>1</sup>, Giuseppe Caliendo <sup>1</sup>,  
Beatrice Severino <sup>1</sup> , Angela Corvino <sup>1,\*</sup> and Ferdinando Fiorino <sup>1</sup>

<sup>1</sup> Dipartimento di Farmacia, Università degli Studi di Napoli “Federico II”, Via D. Montesano 49, 80131 Napoli, Italy

<sup>2</sup> Dipartimento di Farmacia, Università di Pisa, Via Bonanno 6, 56126 Pisa, Italy

<sup>3</sup> Dipartimento di Sanità Pubblica, Università Degli Studi di Napoli Federico II, Via Pansini 5, 80131 Napoli, Italy

\* Correspondence: angela.corvino@unina.it; Tel.: +39-(081)-678618

**Abstract:** Glaucoma is a group of eye diseases consisting of optic nerve damage with corresponding loss of field vision and blindness. Hydrogen sulfide (H<sub>2</sub>S) is a gaseous neurotransmitter implicated in various pathophysiological processes. It is involved in the pathological mechanism of glaucomatous neuropathy and exerts promising effects in the treatment of this disease. In this work, we designed and synthesized new molecular hybrids between antiglaucoma drugs and H<sub>2</sub>S donors to combine the pharmacological effect of both moieties, providing a heightened therapy. Brinzolamide, betaxolol and brimonidine were linked to different H<sub>2</sub>S donors. The H<sub>2</sub>S-releasing properties of the new compounds were evaluated in a phosphate buffer solution by the amperometric approach, and evaluated in human primary corneal epithelial cells (HCEs) by spectrofluorometric measurements. Experimental data showed that compounds **1c**, **1d** and **3d** were the hybrids with the best properties, characterized by a significant and long-lasting production of the gasotransmitter both in the aqueous solution (in the presence of L-cysteine) and in the intracellular environment. Because, to date, the donation of H<sub>2</sub>S by antiglaucoma H<sub>2</sub>S donor hybrids using non-immortalized corneal cells has never been reported, these results pave the way to further investigation of the potential efficacy of the newly synthesized compounds.

**Keywords:** glaucoma; hydrogen sulfide; H<sub>2</sub>S donors; antiglaucoma drugs; molecular hybrids



**Citation:** Sparaco, R.; Citi, V.; Magli, E.; Martelli, A.; Piragine, E.; Calderone, V.; Andreozzi, G.; Perissutti, E.; Frecentese, F.; Santagada, V.; et al. Design, Synthesis and Evaluation of Novel Molecular Hybrids between Antiglaucoma Drugs and H<sub>2</sub>S Donors. *Int. J. Mol. Sci.* **2022**, *23*, 13804. <https://doi.org/10.3390/ijms232213804>

Academic Editor: Antonio Rescifina

Received: 4 October 2022

Accepted: 5 November 2022

Published: 9 November 2022

**Publisher's Note:** MDPI stays neutral with regard to jurisdictional claims in published maps and institutional affiliations.



**Copyright:** © 2022 by the authors. Licensee MDPI, Basel, Switzerland. This article is an open access article distributed under the terms and conditions of the Creative Commons Attribution (CC BY) license (<https://creativecommons.org/licenses/by/4.0/>).

## 1. Introduction

The glaucomas are a group of eye diseases characterized by damage of the optic nerve with corresponding loss of field vision [1]. Glaucoma is the leading cause of irreversible blindness and, to date, 11 million people went blind because of this disease [2]. With advancing age, the likelihood of developing glaucoma is higher; therefore, due to the rapid increase in aging population, by 2040 the number of individuals with glaucoma is projected to grow up to 111.8 million [3].

Although the main cause of this neuropathy is unknown and the pathogenesis is not completely understood, intraocular pressure (IOP) is the major modifiable risk factor and is regulated by the balance of aqueous humor (AH) production and outflow. In a healthy human eye, under steady-state conditions, IOP ranges from 10 to 21 mmHg [4]. Usually, in patients with glaucoma, there is an increase in IOP due to a reduced outflow facility of aqueous humor [5].

Glaucomas can be classified into open-angle glaucoma (OAG) and angle-closure glaucoma (ACG) [1,5–9]. In eyes with open-angle glaucoma, there are no clinically visible perturbations in the eye and the aqueous humor is free to leave the globe; in contrast, with angle-closure glaucoma, the AH drainage is anatomically reduced or blocked [6].

In addition to elevated intraocular pressure, there are common risk factors for the development of glaucomas, such as age, ethnicity, family history of glaucoma, systemic hypertension and diabetes mellitus [5,10,11].

Treatment of glaucoma neuropathies aims to reduce IOP, and on the basis of causes, risk factors, severity and type of glaucoma, different medical options such as topical therapy, oral therapy, surgery or laser procedure are available. First-line treatment consists of the topical application through eye drops of IOP-lowering drugs in monotherapy or as drug combinations. Different classes of medications are used to treat glaucoma, and they either increase the outflow of AH from the eye (prostaglandin analogs and cholinomimetics) or reduce its formation ( $\alpha_2$ -adrenergic agonists,  $\beta$ -adrenergic antagonists and carbonic anhydrase inhibitors) [5,7].

H<sub>2</sub>S is a colorless, flammable and pungent gas and it has been recognized as a third endogenous gasotransmitter, besides nitric oxide (NO) and carbon monoxide (CO) [12]. Several studies have shown that it plays a role in different physiopathological processes; for example, it acts as cardioprotective agent [13], modulates inflammation [14], reduces oxidative stress [15], induces bronchial relaxation [16] and provides a cytoprotective effect [17].

Despite the interesting properties of H<sub>2</sub>S in the human body, as a gaseous compound, it cannot be considered an ideal drug. For this reason, scientists worked on the development of molecules able to release endogenously H<sub>2</sub>S (named H<sub>2</sub>S donors), that could be used as biological instruments and potential drugs [13]. The most promising H<sub>2</sub>S-releasing compounds are the synthetic donors, characterized by an enhanced safety profile and a better pharmacokinetic profile that mimic the time course of the physiologic H<sub>2</sub>S release.

The discovery of the enzymes that mediate H<sub>2</sub>S production in ocular tissues suggested a potential physiological role for this gasotransmitter in the eye [18]. Different ocular diseases related to retinal degeneration like glaucoma, AMD (age-related macular degeneration) and DR (diabetic retinopathy) are characterized by the reduction of endogenous H<sub>2</sub>S levels and expression of H<sub>2</sub>S synthetizing enzymes [19]. Several studies have shown that exogenous H<sub>2</sub>S released by molecular donors can reduce RGCs' damage related to oxidative stress and elevated hydrostatic pressure [15,20–23]. The vasorelaxant effect associated with H<sub>2</sub>S has also been widely demonstrated in ocular vasculature, improving blood flow in the eye [15,21]. In addition, H<sub>2</sub>S plays a role in ocular structures implicated in AH production and outflow as well as in IOP control [18].

In the last decades, H<sub>2</sub>S-releasing molecules have been linked to several pharmaceutical active compounds to synthesize novel molecular hybrids with the purpose of associating the functionality of the parent drugs and endogenous H<sub>2</sub>S. An interesting example of an antiglaucoma drug conjugated to a H<sub>2</sub>S donor is ACS67, a molecular hybrid of latanoprost acid and ADT-OH, a derivative of anethole dithiolethione. Studies confirmed the potentiality of this drug that combines the IOP-lowering effect of latanoprost and the neuroprotective activity of H<sub>2</sub>S, released by ADT-OH [24].

On the basis of the data reported above, and considering the expertise of our research group in the field of H<sub>2</sub>S donors and their applications to synthesize novel chemical entities [25–28], in this experimental work we designed, synthesized and characterized new molecular hybrids between drugs for the treatment of glaucoma and H<sub>2</sub>S-donating moieties. The aim was to synthesize a compound which combines the action of antiglaucomatous drugs and H<sub>2</sub>S released by donors. The idea was to enhance the efficacy of the IOP-lowering medications with the promising effect of H<sub>2</sub>S to provide a heightened therapy. The molecular hybrids must be stable enough to be administered, but once absorbed in the eye they undergo in vivo metabolic reactions that trigger the disintegration of the hybrids, allowing the antiglaucoma drug and the H<sub>2</sub>S donor to interact with their biological targets. By the application of these new entities, we expect a reduction in the administered dosage and side effects.

For the synthesis of the new molecular hybrids, amongst the different classes of antiglaucomatous drugs, brinzolamide ((4R)-4-(ethylamino)-2-(3-methoxypropyl)-1,1-dioxo-3,4-dihydrothieno[3,2-e]thiazine-6-sulfonamide), betaxolol (1-[4-[2-(cyclopropylmethoxy)ethyl]

phenoxy]-3-(propan-2-ylamino)propan-2-ol) and brimonidine (5-bromo-N-(4,5-dihydro-1H-imidazol-2-yl)quinoxalin-6-amine) were selected as native compounds for their higher reactivity and affordable cost. These parent agents were linked to the effective H<sub>2</sub>S-releasing molecules already described, such as 4-hydroxybenzothioamide (TBZ) [29], 5-(4-hydroxyphenyl)-3H-1,2-dithiole-3-thione (ADT-OH) [24,25,28], S-ethyl 4-hydroxybenzodithioate (HBTA) [27] and 4-hydroxyphenyl isothiocyanate (HPI) [30]. In addition, an acetic or succinic spacer was introduced as a linker between the two parts to facilitate the formation of the hybrid.

## 2. Chemistry

Chemical structures of compounds **1a–1d**, **2a–2d** and **3a–3d** are represented in Table 1. The synthetic routes for the synthesis of molecular hybrids of brinzolamide (**1a–1d**), betaxolol (**2a–2d**) and brimonidine (**3a–3d**) are summarized, respectively, in Schemes 1–3.

**Table 1.** Chemical structures of new molecular hybrids between antiglaucoma drugs and H<sub>2</sub>S donors. Values of C<sub>max</sub> (μM) relative to H<sub>2</sub>S generation following the incubation in the assay buffer of the free H<sub>2</sub>S donors (**7–10**) and antiglaucoma hybrids (**1a–1d**, **2a–2d** and **3a–3d**) at concentration of 100 μM, in the presence (+ L-Cys) and in the absence (– L-Cys) of L-cysteine 4 mM; n.d. = not detected (H<sub>2</sub>S release < 0.4 μM). Data are reported as means ± SEM.

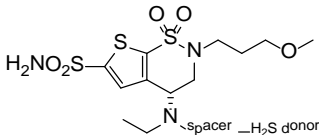
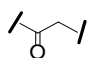
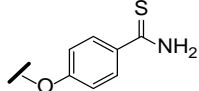
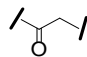
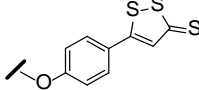
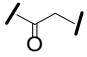
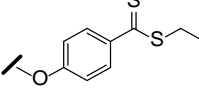
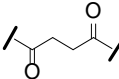
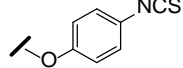
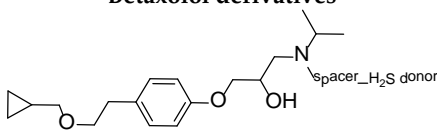
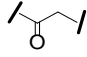
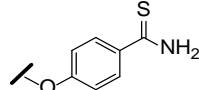
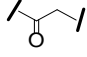
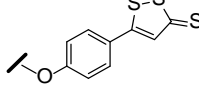
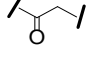
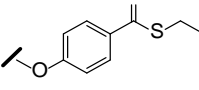
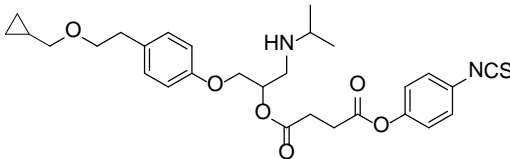
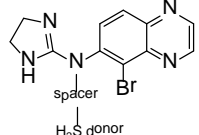




Cmpd	Spacer	H <sub>2</sub> S Donor	H <sub>2</sub> S Release (μM)	
			+ L-Cys	– L-Cys
<b>Brinzolamide Derivatives</b>				
				
<b>1a</b>			0.4 ± 0.2	n.d.
<b>1b</b>			0.9 ± 0.3	0.4 ± 0.1
<b>1c</b>			3.5 ± 0.3	n.d.
<b>1d</b>			2.1 ± 0.4	0.4 ± 0.1
<b>Betaxolol derivatives</b>				
				
<b>2a</b>			0.5 ± 0.2	n.d.
<b>2b</b>			n.d.	n.d.
<b>2c</b>			0.5 ± 0.1	n.d.

Table 1. Cont.

2d		0.5 ± 0.1	n.d.
<b>Brimonidine derivatives</b>			
			
3a		1.2 ± 0.5	n.d.
3b		0.9 ± 0.4	n.d.
3c		1.7 ± 0.5	n.d.
3d		6.2 ± 0.5	0.8 ± 0.1
<b>H<sub>2</sub>S release (μM)</b>			
	+ L-Cys		– L-Cys
TBZ (7)	1.6 ± 0.3		n.d.
ADT-OH (8)	1.8 ± 0.5		1.1 ± 0.3
HBTA (9)	3.5 ± 0.5		n.d.
HPI (10)	15 ± 0.2		3.4 ± 0.7

The general procedure for the synthesis of compounds **1a–1c** and **2a–2c** is as follows: brinzolamide **1** or betaxolol **2** solubilized in DMF were condensed with the H<sub>2</sub>S donors previously conjugated to an acetic spacer (compounds **7b–9b**), by TBTU coupling in the presence of HOBT and N,N-diisopropylethylamine.

The synthesis of compound **1d** started from the conversion of brinzolamide in its succinic derivative **4** by treatment with succinic anhydride in acetonitrile. The following coupling reaction of intermediate **4**, solubilized in DMF, with HPI **10** was performed using TBTU, HOBT and N,N-diisopropylethylamine as coupling agents.

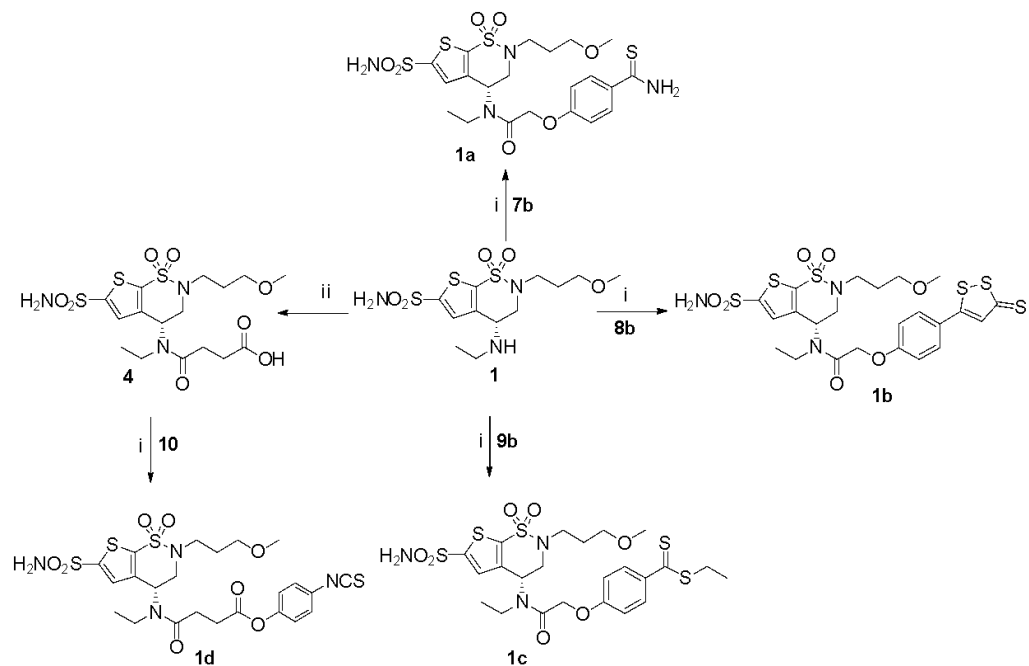
Unlike compounds **2a–2c**, for compound **2d**, the spacer-H<sub>2</sub>S donor moiety is linked to the alcoholic function of betaxolol by an ester bond, instead of to the aminic group, due to the unsuccessful reaction between HPI and tert-butyl bromoacetate. In this case, betaxolol **2** was treated with an excess of succinic anhydride and a catalytic amount of DMAP in anhydrous CH<sub>2</sub>Cl<sub>2</sub> to produce the corresponding hemisuccinated ester that was linked to HPI **10** in the presence of EDAC·HCl and DMAP, obtaining the compound **2d**.

Via one-pot reaction, brimonidine **3** solubilized in anhydrous DMF was first converted into its derivative **5** by treatment with succinic anhydride and DMAP, and then the obtained intermediate was linked to the H<sub>2</sub>S donors (**7–10**) by means of EDAC·HCl and DMAP, producing the corresponding compounds **3a–3d**.

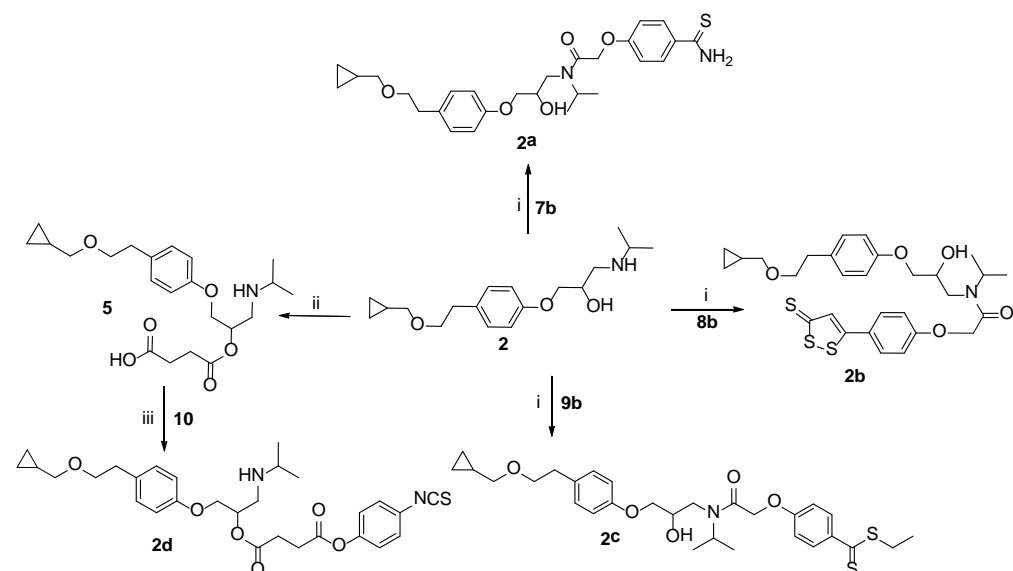
The H<sub>2</sub>S-releasing moieties **7** and **10** were commercially available. ADT-OH **8** was synthesized by reacting trans-anethole and sulfur in DMF according to a process reported in

the literature [31]. The H<sub>2</sub>S donor HBTA **9** was obtained following the synthetic procedure described by our research group [27].

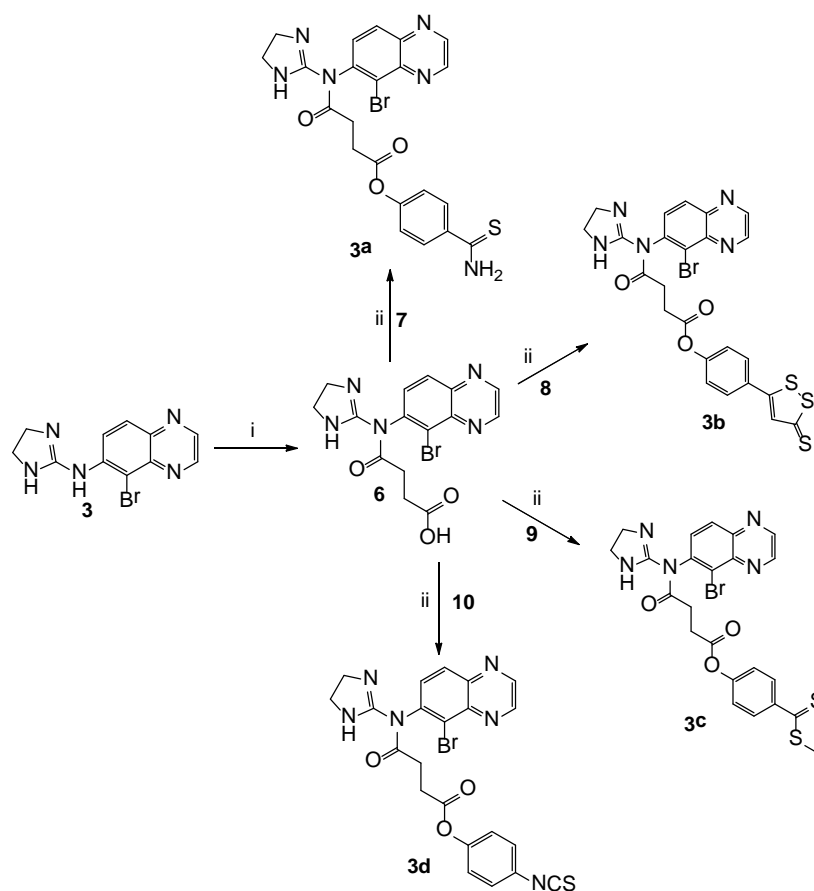
Scheme 4 reports the synthetic route for introducing an acetic spacer on the H<sub>2</sub>S donors **7–9**. TBZ, ADT-OH and HBTA were reacted with tert-butyl bromoacetate in the presence of NaH in DMF to produce intermediates **7a–9a**, which were successfully deprotected by treatment with a 10% (*v/v*) TFA solution in CH<sub>2</sub>Cl<sub>2</sub> affording the desired intermediates **7b–9b**.



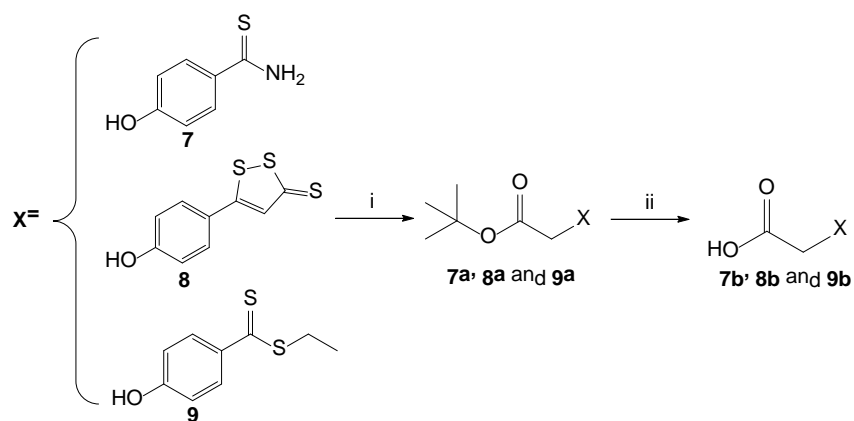
**Scheme 1.** Synthesis of molecular hybrids of Brinzolamide (**1a–1d**). Reagents and conditions: (i) TBTU (1.2 eq.), HOBT (1.2 eq.), DIPEA (2 eq.), DMF, rt, 12 h. (ii) Succinic anhydride (1.1 eq.), ACN, reflux, 12 h.



**Scheme 2.** Synthesis of molecular hybrids of Betaxolol (**2a–2d**). Reagents and conditions: (i) TBTU (1.2 eq.), HOBT (1.2 eq.), DIPEA (2 eq.), DMF, rt, 12 h. (ii) Succinic anhydride (1.5 eq.), DMAP (0.1 eq.), anhydrous DCM, rt, 6h. (iii) EDAC·HCl (1.5 eq.), DMAP (1.5 eq.), anhydrous THF, rt, 12 h.



**Scheme 3.** Synthesis of molecular hybrids of Brimonidine (3a–3d). Reagents and conditions: (i) succinic anhydride (1.1 eq.), DMAP (0.1 eq.), anhydrous DMF, rt, 12 h. (ii) EDAC·HCl (1.5 eq.), DMAP (1.5 eq.), anhydrous DMF, rt, 12 h.



**Scheme 4.** Synthesis of H<sub>2</sub>S-donor derivatives. Reagents and conditions: (i) tert-butyl bromoacetate (1.2 eq.), NaH (1 eq.), DMF, rt, 12 h.; (ii) 10% (v/v) TFA in anhydrous DCM, rt.

### 3. Results and Discussion

#### 3.1. Amperometric Evaluation of H<sub>2</sub>S Release

The H<sub>2</sub>S-generating properties of the compounds **1a–1d**, **2a–2d** and **3a–3d** were evaluated by amperometry, allowing a “real time” detection of the released H<sub>2</sub>S with high sensitivity and selectivity [32]. The assay was performed in an aqueous phosphate buffer, in the absence or in the presence of L-cysteine, whose thiol group mimics the endogenous free thiols in the cells. In Table 1, the C<sub>max</sub> values are reported, representing the highest concentration of H<sub>2</sub>S (μM) recorded during the experiments and released by the H<sub>2</sub>S donating moieties and molecular hybrids (100 μM) in the experimental conditions.

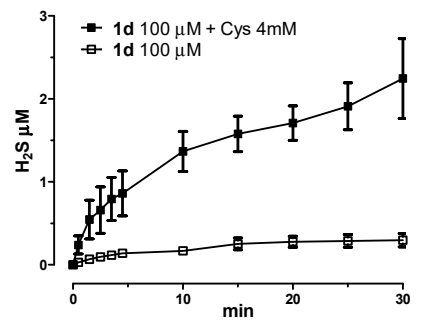
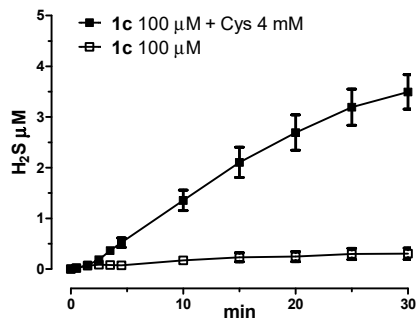
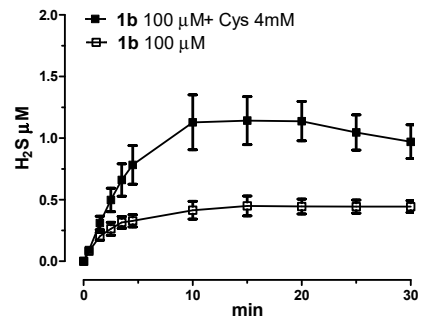
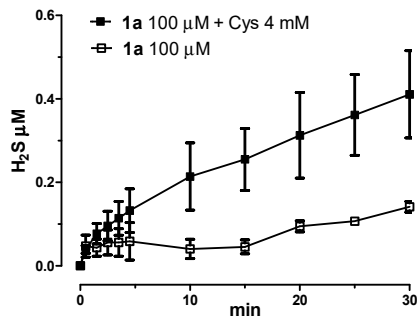
As illustrated in Figure 1, the amperometric assay demonstrated that in the absence of L-cysteine, all the compounds had a completely negligible release of H<sub>2</sub>S (<0.4 μM), except ADT-OH **8** and HPI **10**. These data proved that the presence of a thiol group activates and/or enhances the H<sub>2</sub>S generation from the tested compounds. Therefore, they act as “smart H<sub>2</sub>S donors” since these agents can donate the gaseous transmitter only in a biological environment, i.e., in the presence of organic thiols [26,32,33]. Otherwise, ADT-OH **8** and HPI **10** were able to release H<sub>2</sub>S both in the absence and in the presence of L-cysteine, due to their susceptibility to both a hydrolytic and thiol-dependent mechanism of release.

All brinzolamide hybrids (compounds **1a–1d**) showed an L-cysteine-dependent generation of H<sub>2</sub>S. Nevertheless, the hybrid brinzolamide–TBZ (**1a**) had the lowest release (C<sub>max</sub> = 0.4 ± 0.2 μM) while the compound **1c** (brinzolamide–HBTA) showed a slow and considerable production of H<sub>2</sub>S and within the series of the brinzolamide hybrids, demonstrated the highest C<sub>max</sub> (3.5 ± 0.3 μM). Amperometric data obtained from **1c** confirmed the promising results collected by our research group [27], suggesting HBTA as an innovative and effective thiol-triggered H<sub>2</sub>S donor.

The molecular hybrids synthesized, starting from betaxolol (**2a–2d**), had a weak H<sub>2</sub>S release, enhanced by the presence of L-cysteine. The curves for H<sub>2</sub>S release vs. time in the absence or in the presence of L-Cys for compound **2a** (betaxolol–TBZ) were almost overlapping.

Compounds **3a–3d** required the presence of L-Cys to obtain a detectable generation of H<sub>2</sub>S. The hybrid brimonidine–HPI **3d** showed the best releasing profile, with progressive and time-related slow gas donation. The compound **3d** produced a significant H<sub>2</sub>S generation with a C<sub>max</sub> value of 6.2 ± 0.5 μM. In addition, in this case, data from amperometric assay corroborated the studies indicating that isothiocyanates are promising H<sub>2</sub>S donors [32,33]. Furthermore, as illustrated by Lin et al., the endogenous H<sub>2</sub>S release from isothiocyanates occurs in the presence of thiols (mainly GSH or L-Cys). In particular, the authors showed that isothiocyanates react rapidly with the L-Cys to form an adduct, which then undergoes an intramolecular cyclization reaction to finally release H<sub>2</sub>S [34]. In addition, the electronic effect of the substituents linked to the isothiocyanate may influence the H<sub>2</sub>S formation rate.

A



B

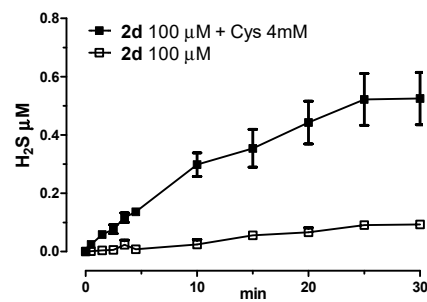
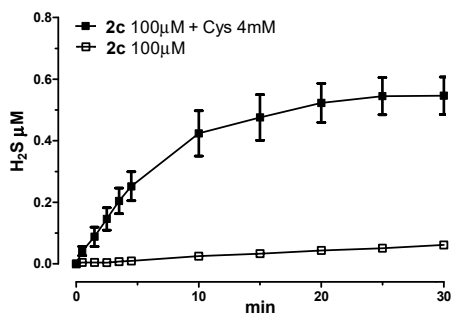
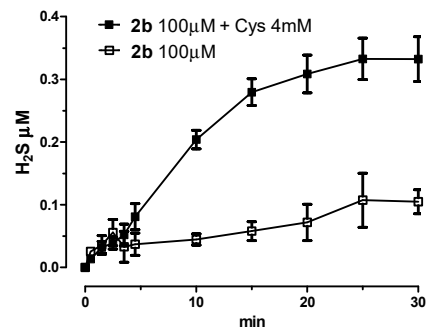
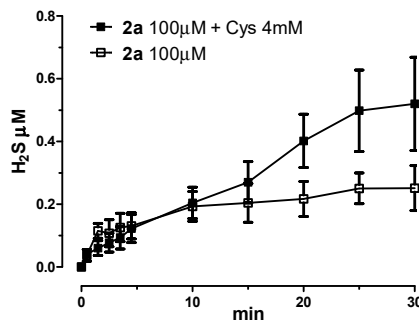
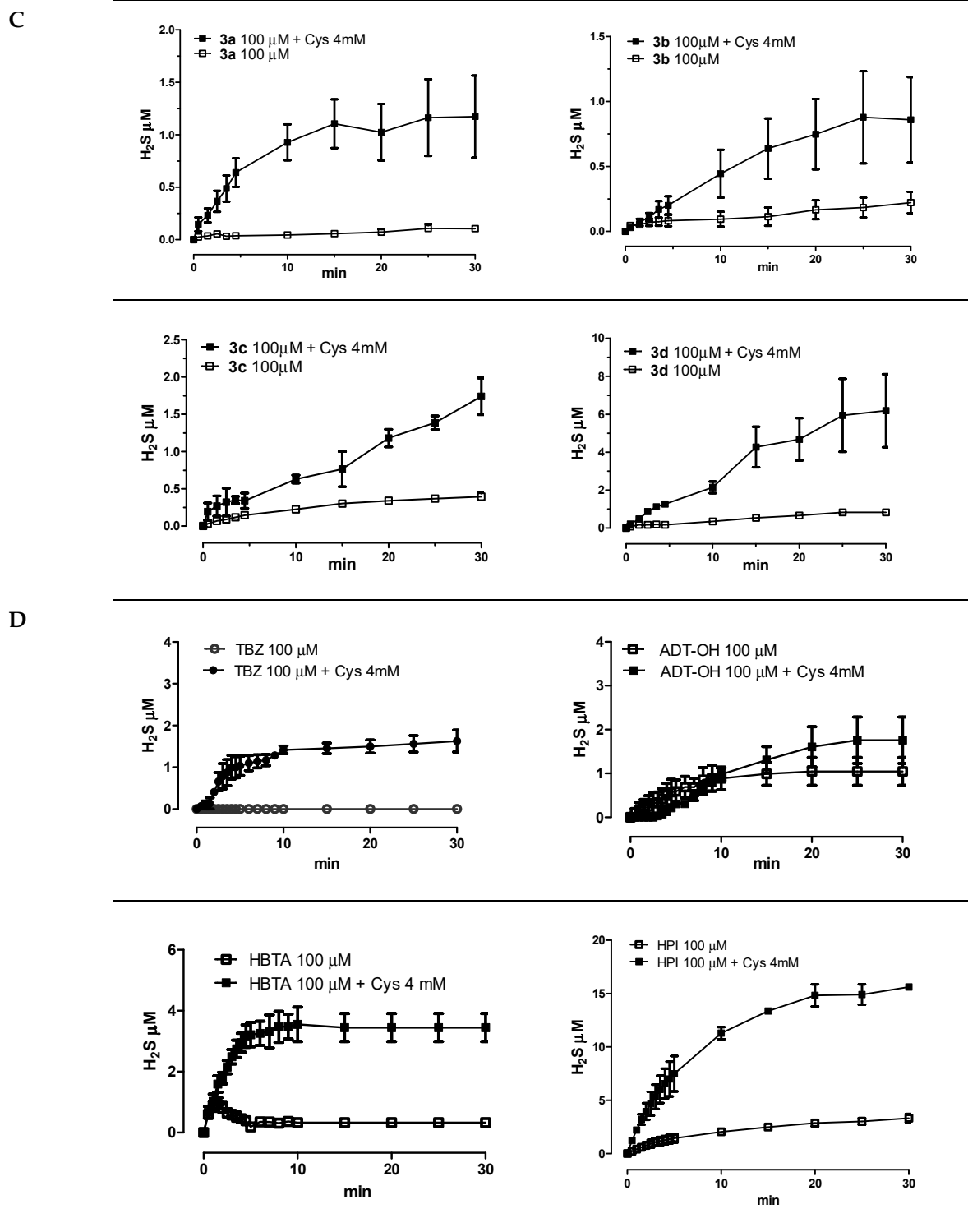


Figure 1. Cont.





**Figure 1.** Curves describe the increase of H<sub>2</sub>S concentration, with respect to time, recorded by amperometry after the incubation of brinzolamide derivatives **1a–1d** (A), betaxolol derivatives **2a–2d** (B), brimonidine derivatives **3a–3d** (C) and the H<sub>2</sub>S donor moieties TBZ, ADT-OH, HBTA, and HPI (D) in the assay buffer, in the absence or in the presence of L-cysteine 4 mM. The vertical bars indicate the SEM.

### 3.2. Intracellular H<sub>2</sub>S Release in HCEs

The H<sub>2</sub>S-releasing properties of the novel molecular hybrids were also tested in human primary corneal epithelial cells (HCEs) to verify the H<sub>2</sub>S formation into the cellular environment without adding any exogenous thiol. This method allows one to understand the behavior of the H<sub>2</sub>S donors in the presence of a physiological level of intracellular L-cysteine, since we use non-immortalized corneal cells.

The detection of intracellular H<sub>2</sub>S was performed by spectrofluorometric measurements using the dye 3'-methoxy-3-oxo-3H-spiro-(isobenzofuran-1,9'-xanthen)-6'-yl-(pyridin-2-yl)disulfanyl benzoate (Washington State Probe-1, WSP-1). WSP-1 can react specifically and irreversibly with H<sub>2</sub>S generated by the tested compounds, releasing a fluorophore detectable with a spectrofluorometer. The increase in the fluorescence compared to the blank is expressed as fluorescence index (FI) [33]. The FI values of the H<sub>2</sub>S donors and the hybrids were compared to the FI value of diallyl disulfide (DADS), considered as reference sulfide donor and responsible for significant H<sub>2</sub>S production ( $p < 0.001$ ). The addition of the vehicle (1% DMSO) in the experimental conditions reflects the endogenous production of H<sub>2</sub>S in the cells.

The experiments were performed in HCEs because the cornea is the major route for topical ocular drug absorption and the corneal epithelium is the most anterior layer of the cornea as well as the main barrier for drug absorption from the tear fluid to the anterior chamber of the eye [35,36].

In Figure 2, H<sub>2</sub>S formation values of the donating moieties (100  $\mu$ M) 7–10 are represented. The compounds TBZ 7 and ADT-OH 8 incubated in HCEs led to a weak and not significant H<sub>2</sub>S-release, almost comparable to that of the vehicle, showing their inability to enter the cell and produce H<sub>2</sub>S. On the other hand, HBTA 9 and HPI 10 promoted an elevated and significant ( $p < 0.001$ ) increase of WSP-1 fluorescence, comparable to the reference H<sub>2</sub>S donor DADS. The graphs reporting the histograms of the intracellular H<sub>2</sub>S release after the incubation of the compounds are subjected to area-under-the-curve analysis of the fluorescence increase monitored for 50 min (For a better characterization and for a better comprehension of the results, see the graphs of the kinetic included in the Supplementary Data).

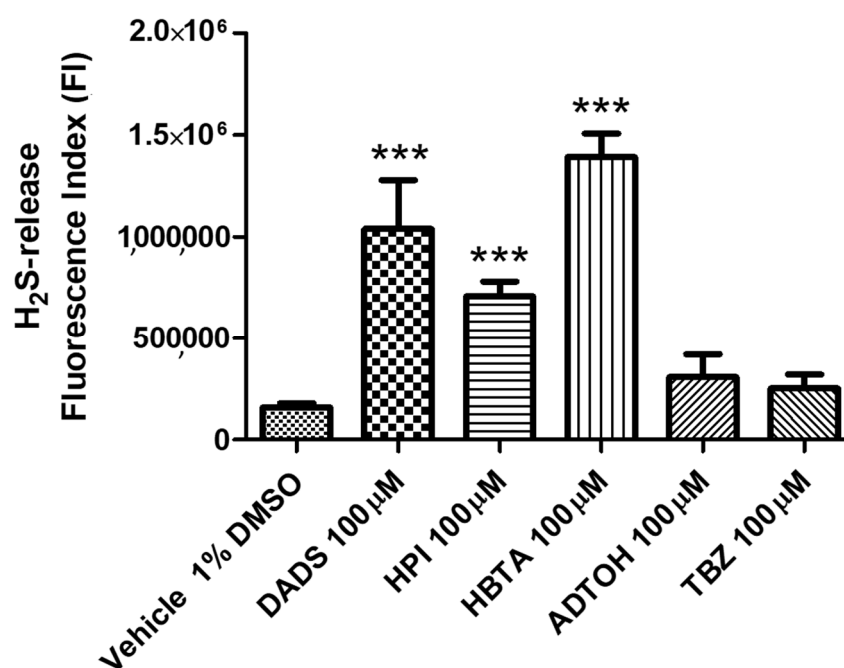


**Figure 2.** Cumulative H<sub>2</sub>S release (expressed as area under the curve of the WSP-1 fluorescence in the recording time) after the incubation of the vehicle, the tested compounds (7–10) and diallyl disulfide (DADS) (100  $\mu$ M). Data were expressed as mean  $\pm$  standard error. Three different experiments were carried out, each in triplicate. ANOVA and Student's *t*-test were applied as statistical analyses; when required, the Bonferroni post hoc test was used to calculate the significance level (\*\*\*)  $p < 0.001$ .

The intracellular H<sub>2</sub>S-releasing profiles of compounds **1a–1d** (100 μM), reported in Figure 3, show that all brinzolamide hybrids evoked a significant H<sub>2</sub>S release. Interestingly, compound **1a** (brinzolamide–TBZ) had an enhanced H<sub>2</sub>S production compared to the TBZ-free moiety. The addition of the hybrid brinzolamide–ADTOH (**1b**) in HCEs caused a higher increase in FI value than ADT–OH by itself. The incubation of compounds **1c** and **1d** (brinzolamide–HBTA and brinzolamide–HPI, respectively) promoted a significant intracellular H<sub>2</sub>S release ( $p < 0.001$ ).

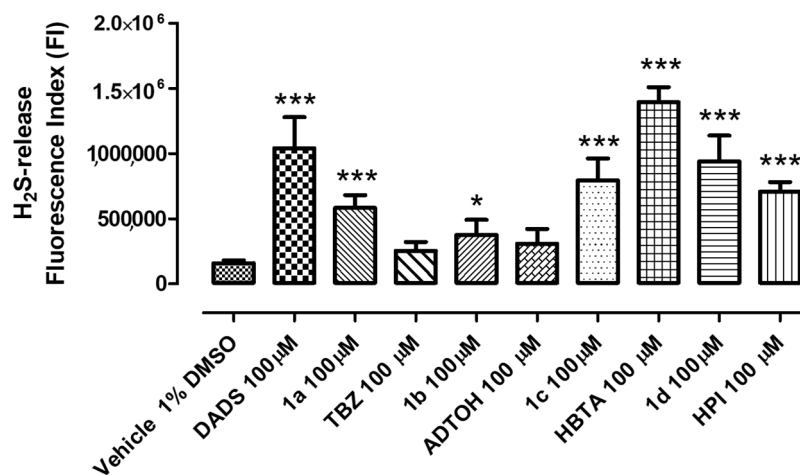


**Figure 3.** Cumulative H<sub>2</sub>S release (expressed as area under the curve of the WSP-1 fluorescence in the recording time) after the incubation of vehicle, the tested compounds (**1a–1d**), the native H<sub>2</sub>S donors and diallyl disulfide (DADS) (100 μM). Data were expressed as mean ± standard error. Three different experiments were carried out, each in triplicate. ANOVA and Student's *t*-test were applied as statistical analyses; when required, the Bonferroni post hoc test was used to calculate the significance level (\*  $p < 0.05$ ; \*\*\*  $p < 0.001$ ).

Compounds **2a** betaxolol–TBZ and **2b** betaxolol–ADTOH did not cause any significant increase in fluorescence (Figure 4). The addition of molecular hybrids betaxolol–HBTA (**2c**) and betaxolol–HPI (**2d**) to WSP-1-preloaded HCEs evoked a mild but significant increase in the intracellular H<sub>2</sub>S levels ( $p < 0.001$ ).

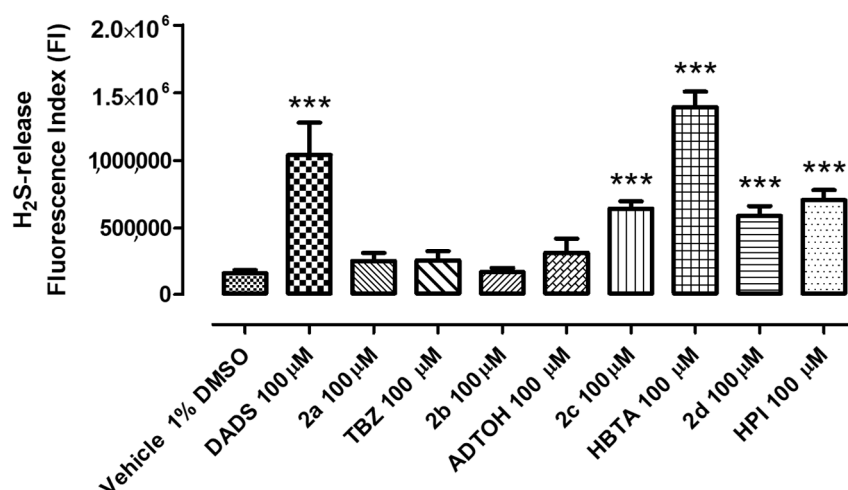


**Figure 4.** Cumulative H<sub>2</sub>S release (expressed as area under the curve of the WSP-1 fluorescence in the recording time) after the incubation of vehicle, the tested compounds (**2a–2d**), the native H<sub>2</sub>S donors and diallyl disulfide (DADS) (100 μM). Data were expressed as mean ± standard error. Three different experiments were carried out, each in triplicate. ANOVA and Student's *t*-test were applied as statistical analyses; when required, the Bonferroni post hoc test was used to calculate the significance level (\*\*\*)  $p < 0.001$ ).

In Figure 5, the results of the fluorometric assay of brimonidine hybrids are graphically represented. All the compounds led to a significant release of hydrogen sulfide ( $p < 0.001$ ), except for the ADT-OH conjugated hybrid (**3b**). Among the compounds **3a–3d**, the molecular hybrid **3d** (brimonidine–HPI) showed the highest increase in fluorescence.

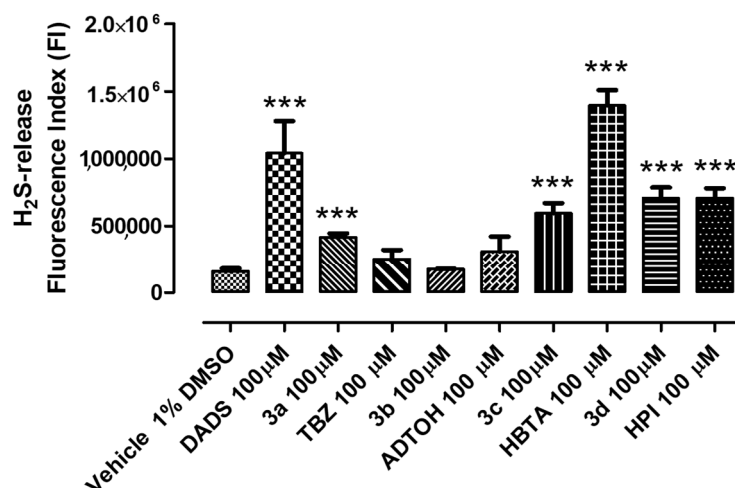


**Figure 5.** Cumulative H<sub>2</sub>S release (expressed as area under the curve of the WSP-1 fluorescence in the recording time) after the incubation of vehicle, the tested compounds (**3a–3d**), the native H<sub>2</sub>S donors and diallyl disulfide (DADS) (100 μM). Data were expressed as mean ± standard error. Three different experiments were carried out, each in triplicate. ANOVA and Student's *t*-test were applied as statistical analyses; when required, the Bonferroni post hoc test was used to calculate the significance level (\*\*\*)  $p < 0.001$ ).

Analyzing the data from the amperometric and the fluorometric assays, the molecular hybrids synthesized by coupling HBTA **9** and HPI **10** with antiglaucoma drugs (**1–3**) released a higher amount of H<sub>2</sub>S in aqueous buffer as well as in the cells, compared to the molecular hybrids of TBZ **7** and ADT-OH **8**. Furthermore, evaluating the influence of the antiglaucoma drugs in the release of H<sub>2</sub>S, betaxolol hybrids demonstrated a weak generation of sulfide when compared to brinzolamide and brimonidine derivatives.

Therefore, compounds **1c**, **1d** and **3d** showed the best releasing profiles, leading to an enhanced H<sub>2</sub>S production. Besides the amount of the gasotransmitter produced, the H<sub>2</sub>S-releasing kinetic also influences biological activity. The amperometric assay demonstrated that these hybrids had a progressive and long-lasting release of H<sub>2</sub>S in the presence of L-cysteine, acting as smart donors. These features are considered as indispensable for the potential clinical application of H<sub>2</sub>S donors, since they avoid the side effects related to a fast release (typical of the sulfide and hydrosulfide salts) and also mimic the endogenous H<sub>2</sub>S production.

## 4. Experimental Section

### 4.1. Materials and Methods

Brinzolamide and brimonidine were purchased from Abcr (Karlsruhe, Germany); betaxolol was purchased from Carbosynth (Compton, UK). All reagents, solvents and other chemicals were commercial products obtained from Merck (Darmstadt, Germany). Melting points, determined using a Buchi Melting Point B-540 instrument (Flawil, Switzerland), are uncorrected and represent values obtained on recrystallized or chromatographically purified material. Spectra of <sup>1</sup>H and <sup>13</sup>C NMR were recorded on a Bruker Advanced 400 MHz spectrometer (Billerica, MA, USA). Spectra of brinzolamide and brimonidine derivatives were recorded in DMSO-*d*<sub>6</sub>. Spectra of betaxolol hybrids were recorded in CD<sub>3</sub>OD and CDCl<sub>3</sub> (compound **2d**). Chemical shifts are reported in ppm. The following abbreviations are used to describe peak patterns when appropriate: s (singlet), d (doublet),

t (triplet), m (multiplet), q (quartet), qt (quintet), dd (doublet of doublet), td (triplet of doublets), bs (broad singlet). Mass spectra of the intermediates and final products were recorded on an LTQ-XL mass spectrometer equipped with a HESI ion source (Thermo Fisher Scientific, Waltham, MA, USA). All reactions were followed by thin-layer chromatography, carried out on Merck silica gel 60 F<sub>254</sub> plates with a fluorescent indicator, and the plates were visualized with UV light (254 nm). Preparative chromatographic purifications were performed using a silica gel column (Kieselgel 60). Solutions were concentrated with a Buchi R-114 rotary evaporator at low pressure.

#### 4.2. Synthesis of Compounds 1a–1d

##### 4.2.1. 2-(4-Carbamothioylphenoxy)-N-ethyl-N-(2-(3-methoxypropyl)-1,1-dioxido-6-sulfamoyl-3,4-dihydro-2H-thieno[3,2-e][1,2]thiazin-4-yl)acetamide (Brinzolamide–TBZ, Compound 1a)

Commercially available brinzolamide **1** (1.00 g; 2.61 mmol) was solubilized in DMF (30 mL) and condensed with the derivative **7b** (0.551 g; 2.61 mmol), via TBTU (1.00 g; 3.13 mmol) and HOBt (0.423 g; 3.13 mmol) in the presence of N,N-diisopropylethylamine (0.910 mL; 5.22 mmol). The mixture was stirred at room temperature for 12 h. The solvent was evaporated and the residue was then purified by silica gel open chromatography using dichloromethane/methanol as eluent (9:1 *v/v*). The compound **1a** was then isolated as a yellowish oil. Yield: 0.628 g; 41.7%.

<sup>1</sup>H NMR (400 MHz, DMSO-*d*<sub>6</sub>) δ: 9.59 (bs, 2H), 9.28 (bs, 2H), 7.88 (d, *J* = 8.5 Hz, 2H), 7.65 (s, 1H), 6.80 (d, *J* = 12.5 Hz, 2H), 4.40 (s, 2H), 4.12–4.10 (m, 1H), 3.87–3.85 (m, 2H), 3.39–3.35 (m, 3H), 3.23 (s, 3H), 3.17–3.15 (m, 1H), 2.83–2.77 (m, 2H), 1.83–1.80 (m, 2H), 1.08 (t, *J* = 7.0 Hz, 3H); <sup>13</sup>C NMR (101 MHz, DMSO-*d*<sub>6</sub>) δ: 199.13, 173.05, 161.67, 151.95, 131.60, 129.62, 128.51, 127.69, 124.95, 119.56, 113.99, 110.13, 69.31, 69.10, 58.40, 54.23, 49.01, 45.84, 29.02. ESI-MS *m/z* [M+H]<sup>+</sup> calculated for C<sub>21</sub>H<sub>28</sub>N<sub>4</sub>O<sub>7</sub>S<sub>4</sub> 576.73, found = 577.2.

##### 4.2.2. N-Ethyl-N-(2-(3-methoxypropyl)-1,1-dioxido-6-sulfamoyl-3,4-dihydro-2H-thieno[3,2-e][1,2]thiazin-4-yl)-2-(4-(3-thioxo-3H-1,2-dithiol-5-yl)phenoxy)acetamide (Brinzolamide–ADTOH, Compound 1b)

Following the synthetic procedure described above for **1a**, compound **1b** was synthesized starting from brinzolamide **1** (1.00 g; 2.61 mmol) and the derivative **8b** (0.742 g; 2.61 mmol), and isolated as an orange solid. Yield: 0.889 g; 52.4%. Mp: 154.1–155.6 °C.

<sup>1</sup>H NMR (400 MHz, DMSO-*d*<sub>6</sub>) δ: 8.2 (bs, 2H), 7.82 (d, *J* = 8.5 Hz, 2H), 7.73 (s, 1H), 6.93 (d, *J* = 12.5 Hz, 2H), 5.76 (s, 1H), 4.47 (s, 2H), 3.94–3.93 (1H, m), 3.63–3.60 (m, 2H), 3.39–3.35 (m, 3H), 3.23 (s, 3H), 3.18–3.14 (m, 1H), 2.89–2.87 (m, 2H), 1.84–1.80 (m, 2H), 1.13 (t, *J* = 7.4 Hz, 3H); <sup>13</sup>C NMR (101 MHz, DMSO-*d*<sub>6</sub>) δ: 215.13, 174.47, 172.87, 162.56, 134.48, 129.21, 128.50, 127.80, 124.98, 123.84, 119.60, 116.05, 110.08, 69.30, 69.13, 58.41, 54.05, 48.78, 45.85, 29.01, 17.20. ESI-MS *m/z* [M+H]<sup>+</sup> calculated for C<sub>23</sub>H<sub>27</sub>N<sub>3</sub>O<sub>7</sub>S<sub>6</sub> 649.87, found = 650.1.

##### 4.2.3. Ethyl 4-(2-(ethyl(2-(3-methoxypropyl)-1,1-dioxido-6-sulfamoyl-3,4-dihydro-2H-thieno[3,2-e][1,2]thiazin-4-yl)amino)-2-oxoethoxy)benzodithioate (Brinzolamide–HBTA, Compound 1c)

Following the synthetic procedure described above for **1a**, compound **1c** was synthesized starting from brinzolamide **1** (1.00 g; 2.61 mmol) and the derivative **9b** (0.670 g; 2.61 mmol), and isolated as a pink solid. Yield: 1.280 g; 78.9%. Mp: 174.0–175.6 °C.

<sup>1</sup>H NMR (400 MHz, DMSO-*d*<sub>6</sub>) δ: 8.19 (bs, 2H), 7.95 (d, *J* = 8.8 Hz, 2H), 7.59 (s, 1H), 6.85 (d, *J* = 12.5 Hz, 2H), 4.43 (s, 2H), 3.83–3.80 (m, 1H), 3.62–3.58 (m, 2H), 3.40–3.34 (m, 5H), 3.21 (s, 3H), 3.15–3.13 (m, 1H), 2.70–2.65 (m, 2H), 1.80–1.78 (m, 2H), 1.31 (t, *J* = 6.1 Hz, 3H), 1.05 (t, *J* = 7.0 Hz, 3H); <sup>13</sup>C NMR (101 MHz, DMSO-*d*<sub>6</sub>) δ: 225.99, 172.69, 163.44, 155.90, 137.46, 128.79, 128.48, 114.81, 110.25, 69.29, 69.15, 58.38, 54.05, 45.82, 43.25, 31.01, 29.02, 18.54, 17.18, 12.84. ESI-MS *m/z* [M+H]<sup>+</sup> calculated for C<sub>23</sub>H<sub>31</sub>N<sub>3</sub>O<sub>7</sub>S<sub>5</sub> 621.83, found = 622.1.

#### 4.2.4. 4-Isothiocyanatophenyl 4-(ethyl(2-(3-methoxypropyl)-1,1-dioxido-6-sulfamoyl-3,4-dihydro-2H-thieno[3,2-e][1,2]thiazin-4-yl)amino)-4-oxobutanoate (Brinzolamide–HPI, Compound **1d**)

The synthesis of compound **1d** occurs in two steps. The first reaction was performed in acetonitrile (20 mL) as solvent, with azeotropic elimination of water from the system [37]. Succinic anhydride (0.287 g; 2.87 mmol) was added to a solution of brinzolamide **1** (1.00 g; 2.61 mmol) and the mixture was stirred overnight at reflux. The solvent was evaporated under reduced pressure and the crude residue was then purified by silica gel open chromatography (dichloromethane/methanol 9:1 *v/v*) to obtain the acid derivative **4** as colorless oil. Yield: 0.891 g; 70.6%. ESI-MS *m/z* [M+H]<sup>+</sup> calculated for C<sub>16</sub>H<sub>25</sub>N<sub>3</sub>O<sub>8</sub>S<sub>3</sub> 483.58, found = 484.4.

In the second step, the synthesized intermediate **4** (1.00 g; 2.07 mmol) was solubilized in DMF (30 mL) and condensed with HPI **10** (0.313 g; 2.07 mmol), by TBTU coupling (0.796 g; 2.48 mmol), in presence of HOBT (0.335 g; 2.48 mmol) and N,N-diisopropylethylamine (0.721 mL; 4.14 mmol). The mixture was stirred at room temperature for 12 h. The solvent was evaporated and the crude material was purified by silica gel open chromatography using ethyl acetate/diethyl ether as eluent (9,5:0,5 *v/v*). Then, the compound **1d** was isolated by crystallization from n-hexane as a white solid. Yield: 0.572 g; 44.8%. Mp: 95.5–96.4 °C.

<sup>1</sup>H NMR (400 MHz, DMSO-*d*<sub>6</sub>) δ: 8.00 (bs, 2H), 7.46 (d, *J* = 8.5 Hz, 2H), 7.25 (s, 1H), 7.17 (d, *J* = 12.5 Hz, 2H), 4.00–3.97 (m, 1H), 3.61–3.58 (m, 2H), 3.47–3.42 (m, 1H), 3.37 (t, *J* = 6.1 Hz, 2H), 3.22 (s, 3H), 3.21–3.18 (m, 1H), 2.83–2.77 (m, 6H), 1.85–1.81 (m, 2H), 0.99 (t, *J* = 7.1 Hz, 3H); <sup>13</sup>C NMR (101 MHz, DMSO-*d*<sub>6</sub>) δ: 171.65, 150.00, 149.12, 142.83, 139.95, 134.15, 129.85, 127.84, 127.70, 127.63, 123.70, 69.25, 58.40, 45.74, 31.42, 29.60, 29.14, 28.60, 22.53, 14.80, 14.43. ESI-MS *m/z* [M+H]<sup>+</sup> calculated for C<sub>23</sub>H<sub>28</sub>N<sub>4</sub>O<sub>8</sub>S<sub>4</sub> 616.75, found = 617.1.

### 4.3. Synthesis of Compounds **2a–2d**

#### 4.3.1. 2-(4-Carbamothioylphenoxy)-N-(3-(4-(2-(cyclopropylmethoxy ethyl)phenoxy)-2-hydroxypropyl)-N-isopropylacetamide (Betaxolol–TBZ, Compound **2a**)

Compound **2a** was obtained according to the procedure reported above for **1a**, starting from betaxolol **2** (1.00 g; 3.25 mmol) and the intermediate **7b** (0.686 g; 3.25 mmol), and isolated as a yellow solid. Yield: 0.511 g; 31.4%. Mp: 73.1–74.5 °C.

The analysis of <sup>1</sup>H, <sup>13</sup>C and bidimensional NMR spectra showed that betaxolol hybrids **2a–2c** are a mixture of *cis/trans* isomers (Figure 6). As reported in details in the literature, unsymmetrically N,N-disubstituted amides are characterized by a hindered rotation around the C(O)–N bond but the energy difference between the two conformations is small and the molecules are a combination of *cis/trans* isomers [38–41]. The rate of conversion between conformational isomers of betaxolol hybrids is sufficiently slow to allow a chemical shift difference of signals arising from *cis* and *trans* isomers.

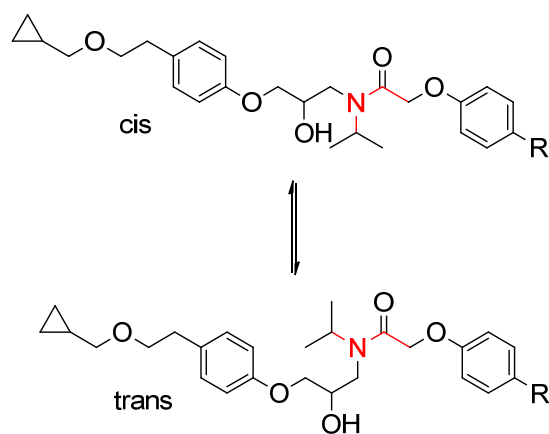


Figure 6. Conformations of betaxolol hybrids.

$^1\text{H}$  NMR (400 MHz,  $\text{CD}_3\text{OD}$ )  $\delta$ : 7.95 (d,  $J = 4.5$  Hz, 2H), 7.92 (d,  $J = 4.6$  Hz, 2H), 7.17 (d,  $J = 4.3$  Hz, 2H), 7.15 (d,  $J = 6.4$  Hz, 2H), 6.99 (d,  $J = 4.4$  Hz, 2H), 6.97 (d,  $J = 4.5$  Hz, 2H), 6.89 (d,  $J = 8.5$  Hz, 2H), 6.83 (d,  $J = 8.6$  Hz, 2H), 5.19 (d,  $J = 15$  Hz, 1H), 4.98 (s, 2H), 4.90 (d,  $J = 14.9$  Hz, 1H), 4.36–4.32 (m, 1H), 4.25–4.17 (m, 2H), 4.04–4.02 (m, 1H), 3.99–3.97 (m, 1H), 3.92–3.94 (m, 1H), 3.87–3.85 (m, 1H), 3.66–3.64 (m, 2H), 3.61 (d,  $J = 5.2$  Hz, 1H), 3.59 (d,  $J = 5.2$  Hz, 1H), 3.55–3.54 (m, 1H), 3.39 (d,  $J = 7.0$  Hz, 1H), 3.37 (d,  $J = 6.9$  Hz, 1H), 3.31 (d,  $J = 3.6$  Hz, 2H), 3.30 (d,  $J = 6.9$  Hz, 2H), 2.80 (td,  $J = 7.1$  Hz, 2.0 Hz, 2H), 1.34 (t,  $J = 6.1$  Hz, 3H), 1.32 (d,  $J = 6.8$  Hz, 3H), 1.28 (d,  $J = 6.6$  Hz, 3H), 1.03–1.00 (m, 1H), 0.49–0.51 (m, 2H), 0.19–0.17 (m, 2H);  $^{13}\text{C}$  NMR (101 MHz,  $\text{CD}_3\text{OD}$ )  $\delta$ : 202.53, 202.40, 171.08, 170.79, 162.86, 158.71, 158.56, 133.97, 133.56, 132.97, 132.64, 131.00, 130.92, 130.59, 130.43, 115.51, 115.45, 115.07, 115.02, 76.60, 72.84, 72.80, 71.44, 71.27, 70.18, 70.12, 67.85, 67.71, 50.48, 49.84, 48.14, 45.78, 36.31, 21.67, 21.28, 20.68, 20.16, 11.40, 3.41. ESI-MS  $m/z$   $[\text{M}+\text{H}]^+$  calculated for  $\text{C}_{27}\text{H}_{36}\text{N}_2\text{O}_5\text{S}$  500.65, found = 501.4.

#### 4.3.2. N-(3-(4-(2-(Cyclopropylmethoxy)ethyl)phenoxy)-2-hydroxypropyl)-N-isopropyl-2-(4-(3-thioxo-3H-1,2-dithiol-5-yl)phenoxy)acetamide (Betaxolol-ADTOH, Compound **2b**)

Compound **2b** was obtained according to the procedure reported above for **1a**, starting from betaxolol **2** (1.00 g; 3.25 mmol) and the intermediate **8b** (0.924 g; 3.25 mmol), and isolated as an orange oil. Yield: 0.699 g; 37.5%.

$^1\text{H}$  NMR (400 MHz,  $\text{CD}_3\text{OD}$ )  $\delta$ : 7.73 (d,  $J = 4.5$  Hz, 2H), 7.48 (d,  $J = 20.4$  Hz, 2H), 7.15 (d,  $J = 8.5$  Hz, 2H), 7.11–7.08 (m, 4H), 7.07 (d,  $J = 4.5$  Hz, 2H), 6.88 (d,  $J = 4.5$  Hz, 2H), 6.78 (d,  $J = 4.6$  Hz, 2H), 5.50 (s, 1H), 5.26 (d,  $J = 15.1$  Hz, 1H), 5.02 (s, 2H), 4.95 (d,  $J = 15$  Hz, 1H), 4.36–4.29 (m, 1H), 4.26–4.15 (1H, m), 4.04–3.95 (1H, m), 3.88–3.78 (1H, m), 3.63 (t,  $J = 7.1$  Hz, 2H), 3.55 (d,  $J = 5.8$  Hz, 1H), 3.50 (q,  $J = 7.0$  Hz, 2H), 3.38 (d,  $J = 6.8$  Hz, 1H), 3.29 (d,  $J = 2.1$  Hz, 2H), 3.27 (d,  $J = 2.1$  Hz, 2H), 2.81–2.78 (m, 2H), 1.35–1.28 (m, 3H), 1.19 (t,  $J = 7.0$  Hz, 3H), 1.04–1.01 (1H, m), 0.53–0.49 (m, 2H), 0.21–0.17 (m, 2H);  $^{13}\text{C}$  NMR (101 MHz,  $\text{CD}_3\text{OD}$ )  $\delta$ : 217.21, 174.88, 174.58, 170.83, 170.53, 163.41, 162.93, 158.70, 158.56, 135.81, 135.67, 132.99, 132.65, 130.99, 130.88, 129.85, 129.66, 126.21, 126.14, 125.80, 116.94, 116.88, 115.52, 115.39, 76.59, 72.81, 71.60, 71.25, 70.15, 70.03, 67.86, 67.75, 66.91, 50.50, 49.84, 48.06, 45.63, 38.88, 36.61, 30.89, 30.75, 21.69, 21.27, 20.68, 20.17, 15.43, 11.40, 3.43. ESI-MS  $m/z$   $[\text{M}+\text{H}]^+$  calculated for  $\text{C}_{29}\text{H}_{35}\text{NO}_5\text{S}_3$  573.79, found = 574.31

#### 4.3.3. Ethyl 4-(2-((3-(4-(2-(cyclopropylmethoxy)ethyl)phenoxy)-2-hydroxypropyl)(isopropyl)amino)-2-oxoethoxy)benzodithioate (Betaxolol-HBTA, Compound **2c**)

Compound **2c** was obtained according to the procedure reported above for **1a**, starting from betaxolol **2** (1.00 g; 3.25 mmol) and the intermediate **9b** (0.833 g; 3.25 mmol), and isolated as a pink oil. Yield: 0.816 g; 46.0%.

$^1\text{H}$  NMR (400 MHz,  $\text{CD}_3\text{OD}$ )  $\delta$ : 8.07 (d,  $J = 4.8$  Hz, 2H), 8.04 (d,  $J = 4.8$  Hz, 2H), 7.17 (d,  $J = 6.5$  Hz, 2H), 7.12 (d,  $J = 6.6$  Hz, 2H), 6.98 (d,  $J = 4.8$  Hz, 2H), 6.96 (d,  $J = 4.8$  Hz, 2H), 6.89 (d,  $J = 4.5$  Hz, 2H), 6.82 (d,  $J = 4.4$  Hz, 2H), 5.22 (d,  $J = 14.9$  Hz, 1H), 4.99 (s, 2H), 4.92 (d,  $J = 14.9$  Hz, 1H), 4.38–4.31 (m, 1H), 4.24–4.18 (m, 3H), 4.05–3.95 (m, 2H), 3.94–3.91 (m, 1H), 3.86–3.81 (m, 1H), 3.61 (t,  $J = 7.1$  Hz, 2H), 3.58 (d,  $J = 5.3$  Hz, 1H), 3.54–3.52 (m, 1H), 3.42–3.36 (m, 4H), 3.30 (d,  $J = 3.1$  Hz, 2H), 3.28 (d,  $J = 3.0$  Hz, 2H), 2.82–2.78 (m, 2H), 1.39 (td,  $J = 7.4, 2.0$  Hz, 3H), 1.30–1.35 (m, 6H), 1.28 (d,  $J = 6.6$  Hz, 3H), 1.06–0.99 (m, 1H), 0.53–0.49 (m, 2H), 0.21–0.17 (m, 2H);  $^{13}\text{C}$  NMR (101 MHz,  $\text{CD}_3\text{OD}$ )  $\delta$ : 202.92, 202.59, 170.88, 170.60, 163.94, 163.53, 158.69, 158.53, 140.03, 139.74, 132.94, 132.55, 130.99, 130.90, 129.82, 129.56, 115.50, 115.43, 115.32, 76.58, 72.85, 72.80, 71.43, 71.21, 70.14, 70.07, 67.81, 67.73, 50.47, 49.81, 48.08, 45.72, 36.31, 31.93, 31.85, 21.67, 21.27, 20.69, 20.18, 12.87, 11.40, 3.42. ESI-MS  $m/z$   $[\text{M}+\text{H}]^+$  calculated for  $\text{C}_{29}\text{H}_{39}\text{NO}_5\text{S}_2$  545.75, found = 546.32

#### 4.3.4. 1-(4-(2-(Cyclopropylmethoxy)ethyl)phenoxy)-3-(isopropylamino)propan-2-yl (4-isothiocyanatophenyl) Succinate (Betaxolol-HPI, Compound **2d**)

Betaxolol **2** (1.00 g; 3.25 mmol), solubilized in anhydrous dichloromethane (30 mL), was treated with a catalytic amount of DMAP (0.040 g; 0.32 mmol). The solution was cooled to 0 °C, and succinic anhydride (0.488 g; 4.87 mmol) was added with the mixture being stirred at room temperature for 6h. The solvent was concentrated in vacuo and the resulting hemisuccinated ester **5** was isolated by silica gel open chromatography (dichloromethane/methanol 9:1 *v/v*) as an oil. Yield: 0.539 g; 40.7%. ESI-MS *m/z* [M+H]<sup>+</sup> calculated for C<sub>22</sub>H<sub>33</sub>NO<sub>6</sub> 407.50, found = 408.6.

The intermediate **5** (1.00 g; 2.45 mmol) was linked to HPI **10** (0.370 g; 2.45 mmol) using EDAC·HCl (0.703 g; 3.67 mmol) and DMAP (0.448 g; 3.67 mmol) as coupling agents in anhydrous THF (20 mL), for 12 h at room temperature. The solvent was removed to obtain the crude product. The residue was loaded on a silica gel open column and eluted with dichloromethane/ethyl acetate (9.5:0.5 *v/v*). The combined and evaporated fractions produced compound **2d** as a colorless oil. Yield: 0.395 g; 29.8%.

<sup>1</sup>H NMR (400 MHz, CDCl<sub>3</sub>) δ: 7.22 (d, *J* = 4.5 Hz, 2H), 7.13 (d, *J* = 8.6 Hz, 2H), 7.09 (d, *J* = 4.5 Hz, 2H), 6.83 (d, *J* = 4.7 Hz, 2H), 4.18–4.11 (m, 1H), 4.04–3.93 (m, 2H) 3.83–3.78 (m, 1H), 3.61 (t, *J* = 7.4 Hz, 2H), 3.46 (dd, *J* = 14.7, 1.8 Hz, 2H), 3.28 (d, *J* = 6.9 Hz, 2H), 2.95–2.80 (m, 6H), 2.00 (bs, 1H) 1.29 (d, *J* = 6.7 Hz, 3H), 1.23 (d, *J* = 6.5 Hz, 3H), 1.07–1.03 (m, 1H), 0.55–0.50 (m, 2H), 0.21–0.17 (m, 2H); <sup>13</sup>C NMR (101 MHz, CDCl<sub>3</sub>) δ: 173.76, 171.53, 157.01, 149.49, 136.02, 131.67, 130.04, 128.93, 126.86, 123.04, 114.40, 75.78, 72.32, 71.93, 69.70, 49.18, 46.36, 35.60, 29.61, 28.54, 21.23, 20.83, 10.76, 3.12. ESI-MS *m/z* [M+H]<sup>+</sup> calculated for C<sub>29</sub>H<sub>36</sub>N<sub>2</sub>O<sub>6</sub>S 540.67, found = 541.3.

#### 4.4. Synthesis of Compounds **3a–3d**

##### 4.4.1. 4-Carbamothioylphenyl

##### 4-((5-bromoquinoxalin-6-yl)(4,5-dihydro-1H-imidazol-2-yl)amino)-4-oxobutanoate (Brimonidine-TBZ, Compound **3a**)

A solution of succinic anhydride (0.376 g; 3.76 mmol) and DMAP (0.041 g; 0.34 mmol) solubilized in DMF (10 mL) was added to brimonidine **3** (1.00 g; 3.42 mmol) in anhydrous DMF (5 mL), under a nitrogen atmosphere, at room temperature, and the mixture was stirred overnight. Subsequently, to the obtained intermediate **6** (not isolated), TBZ **7** (0.524 g; 3.42 mmol), EDAC·HCl (0.983 g; 5.13 mmol) and DMAP (0.627 g; 5.13 mmol) were added. The reaction mixture was stirred at room temperature for 12 h. The solvent was removed in vacuo and the residue was purified by column chromatography on silica gel (ethyl acetate/dichloromethane 8:2 *v/v*). The yellow solid **3a** was obtained by recrystallization with diethyl ether. Yield: 0.610 g; 33.8%. Mp: 121.8–123.4 °C.

<sup>1</sup>H NMR (400 MHz, DMSO-*d*<sub>6</sub>) δ: 9.88 (bs, 1H), 9.52 (bs, 1H), 8.95 (s, 1H), 8.83 (s, 1H), 7.99 (d, *J* = 8.5 Hz, 1H), 7.94 (d, *J* = 8.2 Hz, 2H), 7.59 (d, *J* = 8.9 Hz, 1H), 7.15 (d, *J* = 8.5 Hz, 2H), 7.11 (bs, 1H), 3.94–3.93 (m, 2H), 3.54–3.52 (m, 2H), 3.37–3.35 (m, 2H), 2.94–2.92 (m, 2H); <sup>13</sup>C NMR (101 MHz, DMSO-*d*<sub>6</sub>) δ: 199.52, 171.79, 171.69, 153.24, 150.89, 149.89, 146.04, 143.89, 141.83, 140.47, 137.42, 129.36, 129.23, 128.46, 121.60, 115.38, 44.07, 38.93, 32.50, 29.24. ESI-MS *m/z* [M+H]<sup>+</sup> calculated for C<sub>22</sub>H<sub>19</sub>BrN<sub>6</sub>O<sub>3</sub>S 526.04, found = 527.2.

##### 4.4.2. 4-(3-Thioxo-3H-1,2-dithiol-5-yl)phenyl

##### 4-((5-bromoquinoxalin-6-yl)(4,5-dihydro-1H-imidazol-2-yl)amino)-4-oxobutanoate (Brimonidine-ADTOH, Compound **3b**)

Compound **3b** was synthesized following the synthetic route applied for the synthesis of **3a**. Brimonidine **3** (1.00 g; 3.42 mmol) was linked to ADT-OH **8** (0.774 g; 3.42 mmol). The compound **3b** was then isolated as an orange solid. Yield: 0.700 g; 34.1%. Mp 128.1–129.5 °C.

<sup>1</sup>H NMR (400 MHz, DMSO-*d*<sub>6</sub>) δ: 8.94 (s, 1H), 8.83 (s, 1H), 7.99 (d, *J* = 6.0 Hz, 1H), 7.83 (d, *J* = 10 Hz, 2H), 7.59 (d, *J* = 8.6 Hz, 1H), 7.29 (d, *J* = 8.1 Hz, 2H), 7.12 (bs, 1H), 5.70 (s, 1H), 3.94–3.91 (m, 2H), 3.54–3.52 (m, 2H), 3.38–3.35 (m, 2H), 2.95–2.93 (m, 2H); <sup>13</sup>C NMR (101 MHz, DMSO-*d*<sub>6</sub>) δ: 215.96, 173.24, 171.79, 171.62, 154.07, 150.89, 149.90, 146.05, 143.91,



141.83, 140.48, 136.23, 129.31, 129.17, 128.46, 123.51, 123.47, 115.39, 44.08, 38.94, 32.54, 29.30. ESI-MS  $m/z$   $[M+H]^+$  calculated for  $C_{24}H_{18}BrN_5O_3S_3$  598.98, found = 600.1.

#### 4.4.3. 4-((Ethylthio)carbonothioyl)phenyl 4-((5-bromoquinoxalin-6-yl)(4,5-dihydro-1H-imidazol-2-yl)amino)-4-oxobutanoate (Brimonidine–HBTA, Compound **3c**)

Compound **3c** was synthesized following the synthetic route applied for the synthesis of **3a**. Brimonidine **3** (1.00 g; 3.42 mmol) was linked to HBTA **9** (0.678 g; 3.42 mmol). Compound **3c** was then isolated as a pink solid. Yield: 0.869 g; 44.4%. Mp: 160.5–162.1 °C.

$^1H$  NMR (400 MHz, DMSO- $d_6$ )  $\delta$ : 8.94 (s, 1H), 8.83 (s, 1H), 8.02 (d,  $J$  = 8.5 Hz, 2H), 7.99 (d,  $J$  = 8.9 Hz, 1H), 7.60 (d,  $J$  = 8.6 Hz, 1H), 7.25 (d,  $J$  = 7.6 Hz, 2H), 7.11 (bs, 1H), 3.93 (t,  $J$  = 7.7 Hz, 2H), 3.55 (t,  $J$  = 6.0 Hz, 2H), 3.41–3.35 (m, 4H), 2.96–2.90 (m, 2H), 1.35 (t,  $J$  = 7.3 Hz, 3H);  $^{13}C$  NMR (101 MHz, DMSO- $d_6$ )  $\delta$ : 225.4, 171.32, 171.06, 154.18, 150.41, 149.42, 145.56, 143.42, 141.83, 141.36, 140.00, 128.83, 127.98, 127.89, 122.00, 114.90, 43.59, 38.45, 32.02, 31.14, 28.31, 12.13. ESI-MS  $m/z$   $[M+H]^+$  calculated for  $C_{24}H_{22}BrN_5O_3S_2$  571.03, found = 572.2

#### 4.4.4. 4-Isothiocyanatophenyl 4-((5-bromoquinoxalin-6-yl)(4,5-dihydro-1H-imidazol-2-yl)amino)-4-oxobutanoate (Brimonidine–HPI, Compound **3d**)

Compound **3d** was synthesized following the synthetic route applied for the synthesis of **3a**. Brimonidine **3** (1.00 g; 3.42 mmol) was linked to HPI **10** (0.517 g; 3.42 mmol). The compound **3d** was then isolated as a pale yellow solid. Yield: 1.146 g; 63.8%. Mp: 159.0–160.5 °C.

$^1H$  NMR (400 MHz, DMSO- $d_6$ )  $\delta$ : 8.94 (s, 1H), 8.83 (s, 1H), 7.98 (d,  $J$  = 8.9 Hz, 1H), 7.58 (d,  $J$  = 8.9 Hz, 1H), 7.49 (d,  $J$  = 8.7 Hz, 2H), 7.19 (d,  $J$  = 8.7 Hz, 2H), 7.09 (bs, 1H), 3.92 (t,  $J$  = 7.8 Hz, 2H), 3.52 (t,  $J$  = 6.3 Hz, 2H), 3.36 (t,  $J$  = 7.8, 2H), 2.90 (t,  $J$  = 6.2 Hz, 2H);  $^{13}C$  NMR (101 MHz, DMSO- $d_6$ )  $\delta$ : 171.26, 150.41, 149.42, 145.57, 143.42, 141.36, 140.00, 133.66, 128.83, 127.98, 127.39, 127.21, 123.28, 121.60, 116.33, 114.91, 43.59, 38.45, 32.05, 28.74. ESI-MS  $m/z$   $[M+H]^+$  calculated  $C_{22}H_{17}BrN_6O_3S$  524.03, found = 525.1.

### 4.5. Synthesis of Intermediates **7a–9a**

#### 4.5.1. Tert-butyl 2-(4-carbamothioylphenoxy)acetate (**7a**)

In a two-neck flask, sodium hydride (60% dispersion in mineral oil, 0.261 g; 6.53 mmol) was suspended in DMF (10 mL) and the suspension was stirred and cooled to 0 °C. A solution of TBZ **7** (1.00 g; 6.53 mmol) in DMF (2 mL) was added dropwise. After 10 min a solution of tert-butyl bromoacetate (1.16 mL; 7.84 mmol) in DMF (2 mL) was added dropwise. The mixture was stirred at room temperature for 12 h. The solution was concentrated in vacuo and the crude residue was purified by silica gel open chromatography (dichloromethane as eluent) to produce intermediate **7a** as a yellowish solid. Yield: 1.427 g; 81.7%. ESI-MS  $m/z$   $[M+H]^+$  calculated  $C_{13}H_{17}NO_3S$  267.34, found = 268.6.

#### 4.5.2. Tert-butyl 2-(4-(3-thioxo-3H-1,2-dithiol-5-yl)phenoxy)acetate (**8a**)

Compound **8a** was synthesized from ADT-OH **8** (1.00 g; 4.42 mmol) and tert-butyl bromoacetate (0.783 mL; 5.30 mmol) in the presence of NaH (0.177 g; 4.42 mmol), following the procedure adopted for the synthesis of **7a**, and isolated as a brown solid. Yield: 0.957 g; 63.6%. ESI-MS  $m/z$   $[M+H]^+$  calculated  $C_{15}H_{16}O_3S_3$  340.48, found = 342.0.

#### 4.5.3. Tert-butyl 2-(4-((ethylthio)carbonothioyl)phenoxy)acetate (**9a**)

Compound **9a** was synthesized from HBTA (1.00 g; 5.04 mmol) and tert-butyl bromoacetate (0.893 mL; 6.05 mmol) in the presence of NaH (0.202 g; 5.04 mmol), following the procedure adopted for the synthesis of **7a**, and isolated as a pink solid. Yield: 0.821 g; 52.1%. ESI-MS  $m/z$   $[M+H]^+$  calculated  $C_{15}H_{20}O_3S_2$  312.45, found = 313.8.

#### 4.6. General Procedure for the Synthesis of Intermediates 7b–9b

Intermediates **7a–9a** were dissolved in a 10% (*v/v*) TFA solution in anhydrous dichloromethane (10 mL) and stirred at room temperature until the compound was completely deprotected. Solvent was then removed by reduced pressure distillation and the compounds **7b–9b** were obtained by recrystallization with diethyl ether.

##### 4.6.1. 2-(4-Carbamothioylphenoxy)acetic acid (**7b**)

Synthesized from intermediate **7a** and isolated as a yellowish solid. Yield: 91.1%. ESI-MS  $m/z$   $[M+H]^+$  calculated  $C_9H_9NO_3S$  211.24, found = 212.1.

##### 4.6.2. 2-(4-(3-Thioxo-3H-1,2-dithiol-5-yl)phenoxy)acetic acid (**8b**)

Synthesized from intermediate **8a** and isolated as an orange solid. Yield: 95.4%. ESI-MS  $m/z$   $[M+H]^+$  calculated  $C_{11}H_8O_3S_3$  284.37, found = 285.2.

##### 4.6.3. 2-(4-((Ethylthio)carbonothioyl)phenoxy)acetic acid (**9b**)

Synthesized from intermediate **9a** and isolated as a pink solid. Yield: 93.2%. ESI-MS  $m/z$   $[M+H]^+$  calculated  $C_{11}H_{12}O_3S_2$ , found 256.34 = 257.9.

#### 4.7. Amperometric Determination of $H_2S$ Release

The  $H_2S$ -releasing properties of compounds **1a–1d**, **2a–2d** and **3a–3d** were evaluated by amperometry, through an Apollo-4000 Free Radical Analyzer (World Precision Instrument, WPI) detector and  $H_2S$ -selective minielectrodes (ISO- $H_2S$ -2, WPI) endowed with gas-permeable membranes [25]. The experiments were carried out at room temperature. Following the instructions of the manufacturer, a “PBS buffer 10 $\times$ ” was prepared ( $NaH_2PO_4 \cdot H_2O$ , 1.28 g;  $Na_2HPO_4 \cdot 12H_2O$ , 5.97 g; and NaCl, 43.88 g in 500 mL of  $H_2O$ ) and stocked at 4 °C. Immediately before the experiments, the “PBS buffer 10 $\times$ ” was diluted in distilled water (1:10) to obtain the assay buffer (AB); pH was adjusted to 7.4. The  $H_2S$ -selective minielectrode was equilibrated in 2 mL of the AB until the recovery of a stable baseline. Then, 20  $\mu$ L of a dimethyl sulfoxide (DMSO) solution of the tested compounds were added (final concentration, 100  $\mu$ M; final concentration of DMSO in the AB, 1%). The generation of  $H_2S$  was observed for 30 min. When required by the experimental protocol, L-cysteine 4 mM was added, before the  $H_2S$ -releasing molecule. The relationship between the amperometric currents (recorded in pA) and the corresponding concentrations of  $H_2S$  was determined by calibration curves with increasing concentrations of NaHS (1  $\mu$ M, 3  $\mu$ M and 7  $\mu$ M) at pH 4.0. The curves relative to the progressive increase of  $H_2S$  vs. time, following the incubation of the tested compounds, were analyzed by a fitting curve using the software GraphPad Prism 6.0. The parameter of  $C_{max}$  (the highest concentration of  $H_2S$  obtained during the recording time) and  $TCM_{50}$  (time required to reach a concentration =  $\frac{1}{2} C_{max}$ ) were calculated and expressed as mean  $\pm$  standard error from five different experiments. ANOVA and Student's *t*-test were selected as statistical analysis,  $p < 0.05$  was considered representative of significant statistical differences.

#### 4.8. In Vitro Evaluation

##### 4.8.1. Cell Culture

Human primary corneal epithelial cells (HCEs) were grown in corneal epithelial cell basal media supplemented with corneal epithelial cell growth kit components and 1% of 100 units/mL penicillin and 100 mg/mL streptomycin (Sigma Aldrich) in a tissue culture flask at 37 °C in a humidified atmosphere and 5%  $CO_2$ . HCEs were cultured up to about 90% confluence and 24 h before the experiment; the cells were seeded onto a 96-well black plate, clear bottom pre-coated with gelatin 1% (from porcine skin, Sigma Aldrich), at density of  $72 \times 10^3$  per well. Cells were split 1:2 twice a week and used until passage 18.

#### 4.8.2. Evaluation of H<sub>2</sub>S Release on HCEs

After 24 h to allow cell attachment, the medium was replaced and cells were incubated for 30 min in the buffer standard (HEPES, 20 mM; NaCl, 120 mM; KCl, 2 mM; CaCl<sub>2</sub>·2H<sub>2</sub>O, 2 mM; MgCl<sub>2</sub>·6H<sub>2</sub>O, 1 mM; Glucose, 5 mM; and pH, 7.4, at room temperature) containing the fluorescent dye WSP-1 (Washington State Probe-1, 1,3'-methoxy-3-oxo-3H-spiro[isobenzofuran-1,9'-xanthen]-6'yl 2-(pyridin-2-yl)disulfanyl benzoate, Cayman Chemical) at the concentration of 100 μM [33,42]. Then, the supernatant was removed and replaced with a solution of the tested compounds or diallyl disulfide (DADS) as a known H<sub>2</sub>S donor in buffer standard [29]. When WSP-1 reacts with H<sub>2</sub>S, it releases a fluorophore detectable with a spectrofluorometer at excitation and emission wavelengths of 465–515 nm [25,28,33]. The increasing of fluorescence (expressed as fluorescence index = FI) was monitored after 30 min, using a spectrofluorometer (EnSpire, Perkin Elmer).

#### 4.8.3. Statistical Analysis

Experimental data were analyzed by a computer fitting procedure (software: Graph-Pad Prism 6.0) and expressed as mean ± standard error; three different experiments were performed, each carried out in three replicates. ANOVA and Student's *t*-test were selected as statistical analyses; when required, the Bonferroni post hoc test was used. *p* < 0.05 was considered as representative of significant statistical differences.

### 5. Conclusions

For most forms of glaucoma, including normotensive glaucoma, pharmacological treatment is currently based on IOP control through topical medications. However, the last topical agent for glaucoma therapy approved by the Food and Drug Administration (FDA) dates back to more than 20 years ago [43]. Therefore, with the increasing prevalence of glaucoma worldwide, the exigency of new therapies is emerging.

In this work, we synthesized and characterized new molecular hybrids between currently available drugs for glaucoma therapy and H<sub>2</sub>S-releasing compounds to improve the efficacy of antiglaucoma medications and reduce side effects.

We synthesized hybrid derivatives of brinzolamide (carbonic anhydrase inhibitor; compounds **1a–1d**), betaxolol (β-blocker; compounds **2a–2d**) and brimonidine (α<sub>2</sub>-adrenergic agonist; compounds **3a–3d**).

The new molecular entities were tested for their H<sub>2</sub>S-releasing properties via amperometric and fluorometric assays.

In the amperometric studies, all the synthesized hybrids showed a completely negligible H<sub>2</sub>S production in the absence of L-Cys, proving that the thiol group acts as a trigger for the release of the sulfide. Betaxolol hybrids (compounds **2a–2d**) demonstrated poor H<sub>2</sub>S-releasing properties even in the presence of L-Cys. This behaviour was also confirmed in the fluorometric assay.

Amperometric and fluorometric data showed that molecular hybrids of TBZ (**1a–3a**) and ADT-OH (**1b–3b**) had a low release of H<sub>2</sub>S compared to HBTA and HPI derivatives (**1c–3c** and **1d–3d**, respectively). Notably, compounds **1c** (brinzolamide-HBTA), **1d** (brinzolamide-HPI) and **3c** (brimonidine-HPI) were demonstrated to be the best H<sub>2</sub>S-releasing hybrids both in the aqueous solution (in the presence of L-Cys) and in the intracellular environment.

Even if H<sub>2</sub>S reaches low micromolar levels, it is characterized by a hormetic behavior: high concentrations of H<sub>2</sub>S are toxic and H<sub>2</sub>S donors able to donate high amount of H<sub>2</sub>S showed antitumoral activity [27,44]. To obtain benefits from H<sub>2</sub>S donation, the amount of H<sub>2</sub>S should be at low micromolar level, mimicking its physiological production. This low concentration has been demonstrated to activate, for example, Nrf2, to inhibit Nf-kb, and to protect endothelium from harmful stimuli [45–47]. Additionally, as reported in the literature [48], the therapeutic concentration range of H<sub>2</sub>S in the ocular tissues is 100 nM–100 μM.

These preliminary results confirm hybridization as a promising strategy in the drug design process. By the synthesis of a new molecular entity through the combination of two

or more identical or different drugs, with or without a linker, the aim is to enhance the efficacy of the parent agents [49].

Moreover, based on these results, the idea of combining powerful H<sub>2</sub>S donors such as HBTA or HPI with efficacious IOP-lowering drugs such as prostaglandin analogs could be an interesting, novel perspective to obtain novel antiglaucoma drugs.

**Supplementary Materials:** The following supporting information can be downloaded at: <https://www.mdpi.com/article/10.3390/ijms232213804/s1>.

**Author Contributions:** Conceptualization, G.C., V.C. (Vincenzo Calderone) and F.F. (Francesco Frecentese); methodology, R.S. and V.C. (Valentina Citi); validation, A.C., B.S. and A.M.; formal analysis, G.A. and E.P. (Eugenia Piragin); investigation, E.M. and R.S.; resources, E.P. (Elisa Perissutti); data curation, F.F. (Ferdinando Fiorino); writing—original draft preparation, R.S.; writing—review and editing, A.C., B.S. and V.C. (Valentina Citi); supervision, V.S. and F.F. (Ferdinando Fiorino). All authors have read and agreed to the published version of the manuscript.

**Funding:** This research was funded by POR Campania FSE 2014-2020 ASSE III—Ob. Sp. 14 Az. 10.5.2—“Dottorati di Ricerca con Caratterizzazione Industriale”.

**Institutional Review Board Statement:** Not applicable.

**Informed Consent Statement:** Not applicable.

**Acknowledgments:** The authors gratefully acknowledge Paolo Luciano for his assistance in NMR characterization and POR Campania for the financial support.

**Conflicts of Interest:** The authors declare no conflict of interest.

## References

1. Weinreb, R.N.; Aung, T.; Medeiros, F.A. The pathophysiology and treatment of glaucoma: A review. *JAMA* **2014**, *311*, 1901–1911. [[CrossRef](#)] [[PubMed](#)]
2. Allocco, A.R.; Ponce, J.A.; Riera, M.J.; Magurno, M.G. Critical pathway for primary open angle glaucoma diagnosis. *Int. J. Ophthalmol.* **2017**, *10*, 968–972. [[PubMed](#)]
3. Tham, Y.-C.; Li, X.; Wong, T.Y.; Quigley, H.A.; Aung, T.; Cheng, C.-Y. Global prevalence of glaucoma and projections of glaucoma burden through 2040: A systematic review and meta-analysis. *Ophthalmology* **2014**, *121*, 2081–2090. [[CrossRef](#)] [[PubMed](#)]
4. Wang, Y.X.; Xu, L.; Wei, W.B.; Jonas, J.B. Intraocular pressure and its normal range adjusted for ocular and systemic parameters. The Beijing Eye Study 2011. *PLoS ONE* **2018**, *13*, e0196926. [[CrossRef](#)] [[PubMed](#)]
5. Jonas, J.B.; Aung, T.; Bourne, R.R.; Bron, A.M.; Ritch, R.; Panda-Jonas, S. Glaucoma. *Lancet* **2017**, *390*, 2183–2193. [[CrossRef](#)]
6. Cioffi, C.L. *Drug Delivery Challenges and Novel Therapeutic Approaches for Retinal Diseases*; Springer: Berlin/Heidelberg, Germany, 2020.
7. Kang, J.M.; Tanna, A.P. Glaucoma. *Med. Clin. N. Am.* **2021**, *105*, 493–510. [[CrossRef](#)]
8. Foster, P.J.; Buhrmann, R.; Quigley, H.A.; Johnson, G.J. The definition and classification of glaucoma in prevalence surveys. *Br. J. Ophthalmol.* **2002**, *86*, 238–242. [[CrossRef](#)]
9. Hogan, M.J.; Alvarado, J.A.; Weddell, J.E. *Histology of the Human Eye: An Atlas and Textbook*; Saunders: Ann Arbor, MI, USA, 1971.
10. Weinreb, R.N.; Leung, C.K.; Crowston, J.G.; Medeiros, F.A.; Friedman, D.S.; Wiggs, J.L.; Martin, K.R. Primary open-angle glaucoma. *Nat. Rev. Dis. Prim.* **2016**, *2*, 16067. [[CrossRef](#)]
11. Kong, X.; Chen, Y.; Chen, X.; Sun, X. Influence of family history as a risk factor on primary angle closure and primary open angle glaucoma in a Chinese population. *Ophthalmic Epidemiol.* **2011**, *18*, 226–232. [[CrossRef](#)]
12. Wang, R. Two’s company, three’s a crowd: Can H<sub>2</sub>S be the third endogenous gaseous transmitter? *FASEB J.* **2002**, *16*, 1792–1798. [[CrossRef](#)]
13. Corvino, A.; Frecentese, F.; Magli, E.; Perissutti, E.; Santagada, V.; Scognamiglio, A.; Caliendo, G.; Fiorino, F.; Severino, B. Trends in H<sub>2</sub>S-Donors Chemistry and Their Effects in Cardiovascular Diseases. *Antioxidants* **2021**, *10*, 429. [[CrossRef](#)] [[PubMed](#)]
14. Zano, R.C.; Brancaleone, V.; Distrutti, E.; Fiorucci, S.; Cirino, G.; Wallace, J.L. Hydrogen sulfide is an endogenous modulator of leukocyte-mediated inflammation. *FASEB J.* **2006**, *20*, 2118–2120. [[CrossRef](#)] [[PubMed](#)]
15. Feng, Y.; Prokosch, V.; Liu, H. Current Perspective of Hydrogen Sulfide as a Novel Gaseous Modulator of Oxidative Stress in Glaucoma. *Antioxidants* **2021**, *10*, 671. [[CrossRef](#)] [[PubMed](#)]
16. Khattak, S.; Zhang, Q.Q.; Sarfraz, M.; Muhammad, P.; Ngowi, E.E.; Khan, N.H.; Rauf, S.; Wang, Y.Z.; Qi, H.W.; Wang, D.; et al. The Role of Hydrogen Sulfide in Respiratory Diseases. *Biomolecules* **2021**, *11*, 682. [[CrossRef](#)] [[PubMed](#)]
17. Kimura, H. Production and physiological effects of hydrogen sulfide. *Antioxid. Redox Signal.* **2014**, *20*, 783–793. [[CrossRef](#)] [[PubMed](#)]
18. Han, Y.; Shang, Q.; Yao, J.; Ji, Y. Hydrogen sulfide: A gaseous signaling molecule modulates tissue homeostasis: Implications in ocular diseases. *Cell Death Dis.* **2019**, *10*, 293. [[CrossRef](#)]

19. George, A.K.; Homme, R.P.; Stanicic, D.; Tyagi, S.C.; Singh, M. Protecting the aging eye with hydrogen sulfide. *Can. J. Physiol. Pharmacol.* **2021**, *99*, 161–170. [[CrossRef](#)]
20. Huang, S.; Huang, P.; Liu, X.; Lin, Z.; Wang, J.; Xu, S.; Guo, L.; Leung, C.K.-s.; Zhong, Y. Relevant variations and neuroprotective effect of hydrogen sulfide in a rat glaucoma model. *Neuroscience* **2017**, *341*, 27–41. [[CrossRef](#)]
21. Liu, H.; Anders, F.; Thanos, S.; Mann, C.; Liu, A.; Grus, F.H.; Pfeiffer, N.; Prokosch-Willing, V. Hydrogen Sulfide Protects Retinal Ganglion Cells Against Glaucomatous Injury In Vitro and In Vivo. *Investig. Ophthalmol. Vis. Sci.* **2017**, *58*, 5129–5141. [[CrossRef](#)]
22. Li, P.; Liu, H.; Shi, X.; Prokosch, V. Hydrogen Sulfide: Novel Endogenous and Exogenous Modulator of Oxidative Stress in Retinal Degeneration Diseases. *Molecules* **2021**, *26*, 2411. [[CrossRef](#)]
23. Scheid, S.; Goeller, M.; Baar, W.; Wollborn, J.; Buerkle, H.; Schlunck, G.; Lagrèze, W.; Goebel, U.; Ulbrich, F. Hydrogen Sulfide Reduces Ischemia and Reperfusion Injury in Neuronal Cells in a Dose- and Time-Dependent Manner. *Int. J. Mol. Sci.* **2021**, *22*, 10099. [[CrossRef](#)] [[PubMed](#)]
24. Perrino, E.; Uliva, C.; Lanzi, C.; Soldato, P.D.; Masini, E.; Sparatore, A. New prostaglandin derivative for glaucoma treatment. *Bioorg. Med. Chem. Lett.* **2009**, *19*, 1639–1642. [[CrossRef](#)] [[PubMed](#)]
25. Corvino, A.; Citi, V.; Fiorino, F.; Frecentese, F.; Magli, E.; Perissutti, E.; Santagada, V.; Calderone, V.; Martelli, A.; Gorica, E.; et al. H(2)S donating corticosteroids: Design, synthesis and biological evaluation in a murine model of asthma. *J. Adv. Res.* **2022**, *35*, 267–277. [[CrossRef](#)] [[PubMed](#)]
26. Severino, B.; Corvino, A.; Fiorino, F.; Luciano, P.; Frecentese, F.; Magli, E.; Saccone, I.; Di Vaio, P.; Citi, V.; Calderone, V.; et al. 1,2,4-Thiadiazolidin-3,5-diones as novel hydrogen sulfide donors. *Eur. J. Med. Chem.* **2018**, *143*, 1677–1686. [[CrossRef](#)] [[PubMed](#)]
27. Ercolano, G.; De Cicco, P.; Frecentese, F.; Saccone, I.; Corvino, A.; Giordano, F.; Magli, E.; Fiorino, F.; Severino, B.; Calderone, V.; et al. Anti-metastatic Properties of Naproxen-HBTA in a Murine Model of Cutaneous Melanoma. *Front. Pharmacol.* **2019**, *10*, 66. [[CrossRef](#)] [[PubMed](#)]
28. Giordano, F.; Corvino, A.; Scognamiglio, A.; Citi, V.; Gorica, E.; Fattorusso, C.; Persico, M.; Caliendo, G.; Fiorino, F.; Magli, E.; et al. Hybrids between H(2)S-donors and betamethasone 17-valerate or triamcinolone acetonide inhibit mast cell degranulation and promote hyperpolarization of bronchial smooth muscle cells. *Eur. J. Med. Chem.* **2021**, *221*, 113517. [[CrossRef](#)] [[PubMed](#)]
29. Martelli, A.; Testai, L.; Citi, V.; Marino, A.; Pugliesi, I.; Barresi, E.; Nesi, G.; Rapposelli, S.; Taliani, S.; Da Settimo, F.; et al. Arylthioamides as H<sub>2</sub>S Donors: L-Cysteine-Activated Releasing Properties and Vascular Effects in Vitro and in Vivo. *ACS Med. Chem. Lett.* **2013**, *4*, 904–908. [[CrossRef](#)]
30. Citi, V.; Corvino, A.; Fiorino, F.; Frecentese, F.; Magli, E.; Perissutti, E.; Santagada, V.; Brogi, S.; Flori, L.; Gorica, E. Structure-activity relationships study of isothiocyanates for H<sub>2</sub>S releasing properties: 3-Pyridyl-isothiocyanate as a new promising cardioprotective agent. *J. Adv. Res.* **2021**, *27*, 41–53. [[CrossRef](#)]
31. Wallace, J.L.; Cirino, G.; Caliendo, G.; Sparatore, A.; Santagada, V.; Fiorucci, S. Derivatives of 4- or 5-Aminosalicylic Acid. U.S. Patent 7910568, 22 March 2011.
32. Martelli, A.; Citi, V.; Testai, L.; Brogi, S.; Calderone, V. Organic Isothiocyanates as Hydrogen Sulfide Donors. *Antioxid. Redox Signal.* **2020**, *32*, 110–144. [[CrossRef](#)]
33. Martelli, A.; Citi, V.; Calderone, V. Vascular Effects of H(2)S-Donors: Fluorimetric Detection of H(2)S Generation and Ion Channel Activation in Human Aortic Smooth Muscle Cells. *Methods Mol. Biol.* **2019**, *2007*, 79–87.
34. Lin, Y.; Yang, X.; Lu, Y.; Liang, D.; Huang, D. Isothiocyanates as H(2)S Donors Triggered by Cysteine: Reaction Mechanism and Structure and Activity Relationship. *Org. Lett.* **2019**, *21*, 5977–5980. [[CrossRef](#)] [[PubMed](#)]
35. Mannermaa, E.; Vellonen, K.S.; Urtti, A. Drug transport in corneal epithelium and blood-retina barrier: Emerging role of transporters in ocular pharmacokinetics. *Adv. Drug Deliv. Rev.* **2006**, *58*, 1136–1163. [[CrossRef](#)] [[PubMed](#)]
36. Davies, N.M. Biopharmaceutical considerations in topical ocular drug delivery. *Clin. Exp. Pharmacol. Physiol.* **2000**, *27*, 558–562. [[CrossRef](#)] [[PubMed](#)]
37. Scozzafava, A.; Menabuoni, L.; Mincione, F.; Briganti, F.; Mincione, G.; Supuran, C.T. Carbonic anhydrase inhibitors. Synthesis of water-soluble, topically effective, intraocular pressure-lowering aromatic/heterocyclic sulfonamides containing cationic or anionic moieties: Is the tail more important than the ring? *J. Med. Chem.* **1999**, *42*, 2641–2650. [[CrossRef](#)] [[PubMed](#)]
38. Petrović, S.D.; Stojanović, N.D.; Antonović, D.G.; Mijin, D.Ž.; Nikolić, A.D. Conformations of unsymmetrical N-t-butyl-N-substituted 2-phenylacetamides. *J. Mol. Struct.* **1997**, *410–411*, 35–38. [[CrossRef](#)]
39. Isbrandt, L.; Tung, W.C.T.; Rogers, M.T. An NMR study of hindered internal rotation in some unsymmetrically N,N-disubstituted acetamides. *J. Magn. Reson.* **1973**, *9*, 461–466. [[CrossRef](#)]
40. LaPlanche, L.A.; Rogers, M.T. Configurations in Unsymmetrically N,N-Disubstituted Amides. *J. Am. Chem. Soc.* **1963**, *85*, 3728–3730. [[CrossRef](#)]
41. Zheng, Y.; Tice, C.M.; Singh, S.B. Conformational control in structure-based drug design. *Bioorg. Med. Chem. Lett.* **2017**, *27*, 2825–2837. [[CrossRef](#)]
42. Lin, V.S.; Chen, W.; Xian, M.; Chang, C.J. Chemical probes for molecular imaging and detection of hydrogen sulfide and reactive sulfur species in biological systems. *Chem. Soc. Rev.* **2015**, *44*, 4596–4618. [[CrossRef](#)]
43. Dikopf, M.S.; Vajaranant, T.S.; Edward, D.P. Topical treatment of glaucoma: Established and emerging pharmacology. *Expert Opin. Pharmacother.* **2017**, *18*, 885–898. [[CrossRef](#)]

44. Fortunato, S.; Lenzi, C.; Granchi, C.; Citi, V.; Martelli, A.; Calderone, V.; Di Pietro, S.; Signore, G.; Di Bussolo, V.; Minutolo, F. First Examples of H<sub>2</sub>S-Releasing Glycoconjugates: Stereoselective Synthesis and Anticancer Activities. *Bioconj. Chem.* **2019**, *30*, 614–620. [[CrossRef](#)] [[PubMed](#)]
45. Testai, L.; Citi, V.; Martelli, A.; Brogi, S.; Calderone, V. Role of hydrogen sulfide in cardiovascular ageing. *Pharmacol. Res.* **2020**, *160*, 105125. [[CrossRef](#)] [[PubMed](#)]
46. Martelli, A.; Piragine, E.; Gorica, E.; Citi, V.; Testai, L.; Pagnotta, E.; Lazzeri, L.; Pecchioni, N.; Ciccone, V.; Montanaro, R.; et al. The H<sub>2</sub>S-Donor Erucin Exhibits Protective Effects against Vascular Inflammation in Human Endothelial and Smooth Muscle Cells. *Antioxidants* **2021**, *10*, 961. [[CrossRef](#)] [[PubMed](#)]
47. Testai, L.; Pagnotta, E.; Piragine, E.; Flori, L.; Citi, V.; Martelli, A.; Di Cesare Mannelli, L.; Ghelardini, C.; Matteo, R.; Suriano, S.; et al. Cardiovascular benefits of *Eruca sativa* mill. Defatted seed meal extract: Potential role of hydrogen sulfide. *Phytother. Res.* **2022**, *36*, 2616–2627. [[CrossRef](#)] [[PubMed](#)]
48. Susmit, M.; Farvo, C.; Somnath, S. Unmet needs in glaucoma therapy: The potential role of hydrogen sulfide and its delivery strategies. *J. Control. Release* **2022**, *347*, 256–269.
49. Sampath Kumar, H.M.; Herrmann, L.; Tsogoeva, S.B. Structural hybridization as a facile approach to new drug candidates. *Bioorg. Med. Chem. Lett.* **2020**, *30*, 127514. [[CrossRef](#)] [[PubMed](#)]